

## Seiches around the Shetland Islands

D.T. Pugh<sup>1</sup>, P.L. Woodworth<sup>1</sup> and E.M.S. Wijeratne<sup>2</sup>

1. National Oceanography Centre, Joseph Proudman Building, 6 Brownlow Street, Liverpool L3 5DA, United Kingdom

2. Oceans Graduate School & The UWA Oceans Institute, The University of Western Australia, Crawley, Western Australia, 6009, Australia

Correspondence to: P.L. Woodworth ([plw@noc.ac.uk](mailto:plw@noc.ac.uk))

### Abstract

Sea level records have been obtained from a dozen tide gauges deployed around the Shetland Islands, and the high-frequency components of each record have been analysed to determine how the amplitudes and periods of seiches vary from place to place. We have found that seiches occur almost everywhere, although with different periods at different locations, and sometimes with amplitudes exceeding several decimetres. Spectral analysis shows that two or more modes of seiching are present at some sites. The study attempts to explain, with the help of a numerical model, why seiches with particular periods are observed at each location, and what forcings are responsible for them. In particular, we have revisited an earlier study of seiches on the east coast of Shetland by Cartwright and Young (1974) and find no evidence to support the theory that they proposed for their generation. In addition, we have investigated how often and why the largest seiche events occur at Lerwick (with trough-to-crest wave heights of about 1 m), taking advantage of its long sea level record. Seiches (and other types of high-frequency sea level variability) are often ignored in studies of sea level changes and their coastal impacts. And yet they can be large enough to contribute significantly to the extreme sea levels that have major impacts on the coast. Therefore, our Shetland research serves as a case study of the need to have a fuller understanding of the climatology of seiches for the whole world coastline.

Keywords: Coastal seiches; Shelf resonances; Tide gauge measurements; Numerical seiche modelling; Tidal ringing

### 1. Introduction

Tide gauge records from many locations demonstrate high-frequency oscillations in sea level that are superimposed on the tidal curve. Airy (1878) seems to have been the first to observe them, in a tidal record from Swansea in South Wales, and then in charts from a tide gauge in the Grand Harbour in Malta. He noted oscillations in the latter that persisted for several days at a time with an amplitude of approximately 6 inches and a period of about 21 minutes. He referred to them as ‘seiches’, having corresponded with F-A. Forel in Lausanne, who had used that term to describe similar oscillations in Lake Geneva (Forel, 1876, 1901). Seiches were later also the subject of study in Scottish lakes (Chrystal, 1906, 1910).

Coastal seiches have been explained as resonances of harbours, bays or continental shelves. There are many ocean processes which are able to generate long waves that can force such bodies of water resonantly. These include the force of the wind, changes in air pressure (including those which initiate meteotsunamis), the ocean tide, the ocean internal tide, wave energy and tsunamis. In addition, seiches can be initiated by earthquakes and landslides. Many examples are given by Rabinovich (2009).

At some locations, seiches are observed almost continuously due to probably more than one forcing (e.g. Park et al., 2016; Woodworth, 2017). The resonant periods of harbours, inlets and shelves with simple shapes can be determined straightforwardly (Wilson, 1972; Sorensen, 1978), and all such calculations yield periods proportional to the reciprocal of the square root of water depth.

This paper describes the rich collection of seiches around the Shetland Islands, to the north of Scotland (Figure 1a). Shetland consists of three main islands (Mainland in the south, Yell in the middle, and Unst in the north), and a number of smaller ones (such as Out Skerries, Fair Isle and Foula) some distance away, surrounded by shallow continental shelf on all sides (Figure 1b, Flynn, 1973). The islands and the shelf are exposed to strong winds from almost any direction but most frequently from the southwest. Our measurements of seiches were made using permanent and temporary tide gauges at 12 sites (Table 1). In each case, the main periods associated with the seiches have been obtained, and the mechanisms for their generation have been explored as far as possible with the use of an ocean model. The number of times that especially large seiches occur in Shetland has been investigated using over two decades of tide gauge data from Lerwick, together with meteorological information.

It has been known for many years that the Lerwick tide gauge record shows evidence for seiches with a period of about half an hour and a typical amplitude of about 10 cm (Tucker, 1963; Rossiter, 1971). Cartwright and Young (1974) made use of measurements at Lerwick and also further north at Baltasound (Figure 1b), which indicated that the seiches at the two locations were similar in both amplitude and period, leading them to propose a mechanism for their common generation in terms of coherent shelf resonance and coastally-trapped edge waves. This paper uses our more extensive Shetland data set to revisit that suggestion, to see whether it explains the data better than, for example, individual sets of local resonance that happen to be energised by the same storms.

## 2. Tide gauge and meteorological data sets

The main tide gauge in Shetland is at Lerwick on the east coast of the Shetland mainland (Figure 1b). This is a long-established bubbler pressure gauge that is part of the National (or 'A Class') Network operated by the Environment Agency (EA). The main purpose of the gauge is to provide 15-min averages of sea level for use in flood warning by the UK Flood Forecasting Centre, which is operated by the UK Met Office and the EA, as well as in long-term sea level research. These 15-min average values are calculated from individual measurements averaged over each second and may be obtained from the British Oceanographic Data Centre (BODC, <https://www.bodc.ac.uk>). The 1-sec values themselves were not transmitted or archived until March 2015. They were then used by the National Oceanography Centre (NOC) to compute 10-sec values, which were transmitted to the Intergovernmental Oceanographic Commission Sea Level Station Monitoring Facility (SLSMF, <http://www.ioc-sealevelmonitoring.org>), and 1-min average values, the latter being the most suitable for the purposes of this paper. Unfortunately, the provision of such high-rate data from Lerwick to the SLSMF came to an end in March 2018.

We were also provided with data sets of 1-min values of sea level obtained from two gauges operated by Shetland Islands Council. Sella Ness is part of the Sullom Voe oil terminal where data were obtained from a Valeport Model 740 gauge, while Scalloway was equipped with a Valeport Tidemaster. Both are differential (vented) strain gauges.

In addition, at a number of sites we made temporary measurements of subsurface pressure (SSP), the combination of water level pressure plus atmospheric pressure, using Richard Brancker Research (RBR) XR-420 and TGR-1050 strain gauge pressure sensors. Each one was deployed in several metres of water, with a heavy weight attached to hold them to the sea bed, and a rope to enable recovery. The sensors were programmed to make measurements of SSP every 3 minutes integrated over enough

time to average out changes in pressure due to waves (10 seconds was chosen at some sites and 6 seconds at others). SSP is just as suitable as sea level for the measurement of seiches, as there is no significant variability in atmospheric pressure at the seiche frequencies of interest (see below), and SSP is a generally less noisy parameter than real sea level. SSP measured in decibars is treated below as equivalent to 100 mm of sea level. At one further site (Lerwick North), a KPSI-500 differential pressure sensor was used which delivered spot measurements of sea level (and not SSP) every 3 minutes. These temporary deployments were made during three main periods: September-December 2015, December 2015 – April 2016, and April-August 2016 (Table 1).

Meteorological data including one-minute air pressures and winds from the Lerwick weather station were supplied by the UK Met Office, while additional meteorological information was provided by the Centre for Environmental Data Analysis (CEDA, <http://archive.ceda.ac.uk>).

### 3. Seiches observed in the tide gauge data

#### 3.1 Data processing

Each record in Table 1 was analysed using two time series: the measured ‘total’ values of sea level (or SSP), which contain the tide and all non-tidal sea level variability; and values of ‘residuals’, which contain the high-frequency seiche signals. The latter were obtained by filtering the ‘total’ record in a procedure that consists of fits to moving sections of data, each one lunar day (24.84 hours) wide and centred on a particular 1- (or 3-) minute measurement. The data in each section are parameterised using an M1 sinusoid, plus harmonics with 2-12 times its frequency, plus an S2 sinusoid (i.e. 26 terms in all) and an average value over the section, thereby accounting for the tide and lower-frequency components of non-tidal variability with frequencies below approximately 0.5 cph. The data will not be over-fitted as with 1- (or 3-) minute sampling there are always far more data than parameters. A ‘residual’ is then defined for that central 1- (or 3-) minute value by its difference from the parameterisation at that point. The procedure then moves on to place the next ‘total’ measurement at the centre of a new fit.

Figure 2a shows an example of a residual time series from Lerwick. The residuals are usually several tens of mm in magnitude, occasionally 100-200 mm such as at the end of January 2016, and on rare occasions approach 0.5 m as at the start of July 2015. Figure 2b shows the standard deviation of this high-frequency variability within 2-hour sections of data.

The main spectral peaks in the Lerwick record are shown in Figure 2c which is derived from the total series in order to show the full spectrum. However, it starts at 0.1 cph in order to cut off the major diurnal and semidiurnal tides; the line spectrum of tidal components with frequencies larger than semidiurnal can clearly be seen on the left. Otherwise, there is a broad peak centred on 2.14 cph (28.1 min) which is similar to that shown by Cartwright and Young (1974) using earlier data. This is the main frequency of interest to us which, it will be seen, corresponds to either a quarter-wavelength or asymmetric half-wavelength seiche mode of Lerwick Harbour. Not discussed by Cartwright and Young (1974) are other peaks at higher frequency that are probably associated with shorter spatial-scale (e.g. cross-harbour) modes.

Table 2 summarises the main peaks in the spectra at each site above 1 cph (apart from one major peak below 1 cph that we note from Sella Ness). Peaks were identified by summing the power into frequency bins of 0.025 cph (corresponding to bins of 1.5 min in period at 1 cph) and then searching for peaks in power that are further than 0.4 cph away from a larger peak (or 0.3 cph that we decided was a better choice for Toft.) The method appears to work satisfactorily for lower and medium

frequencies but inevitably identifies some spurious peaks as frequency increases. Nevertheless, all peaks identified by this method are listed in Table 2.

Supplementary Figure A(iv, L) shows a wavelet plot made from the residual time series. The '28-min seiche' at Lerwick is persistent throughout the record with periods of higher and lower amplitude corresponding to those in Figure 2(b). Those fluctuations at 28 minutes in the wavelet plot occur at much the same times as those at other frequencies (in particular those around 9 minutes), indicating that different seiche modes are energised at similar times. The Supplementary Material shows that this situation also applies to the wavelet plots from other locations.

Figures for all stations, corresponding to those for Lerwick in Figure 2 and Supplementary Figure A(iv,L), may be found in the Supplementary Information Set A.

### 3.2 Comments on each site

#### (i) Lerwick

Lerwick is situated on the west side of a harbour, approximately 3 km long and 1 km wide, aligned north-south between the Shetland mainland and the island of Bressay. Its depth is ~10 m in the northern half of the harbour and ~20 m in the southern half (below Mean Low Water Springs, NLS, 1927). Several shallow sections are said to be 'dredged to 9m' (LPA, 2018). The main entrance of the harbour is to the south. There is also a narrow northern entrance, approximately 900 m long, 300m wide and ~10 m deep. The long-term bubbler tide gauge is located at the Lerwick lifeboat station near the southwest corner of the harbour, shown by a yellow dot in Figure 1(c).

The residuals from the Lerwick record have been described in the previous section. Confirmation that the 28-min seiche is produced in the harbour comes from a 'window-regression' analysis similar to that of Woodworth et al. (2005), in which the residuals are analysed in separate 6-hour windows centred on each data point in the record. The residuals in the window are parameterized in terms of a quadratic time dependence, so as to remove any long-term background components, plus a simple cosine term to represent the seiche component, allowing values of seiche period between 50-150% of the nominal period (28 minutes in this case). One result is a time series of seiche amplitude throughout the record (Figure 3). An obvious objection to this method is that the seiche signal might not be stationary through the window. However, from comparison of the amplitudes computed by this analysis to those evident in the original record (Figure 2), we believe that the method does describe well the variations in seiche amplitude and, given that several cycles of seiche will occur during the window, then the period should be reasonably well measured also.

If the seiche period ( $T$ ) depends upon  $1/\sqrt{h}$ , where  $h$  is depth, then in principle one should be able to estimate the effective depth ( $H$ ) of the body of water in which the seiche is generated by examining how  $T$  varies with the height of the tide, assuming that the effective length of the water body does not also change i.e.  $H = -0.5 T/(\partial T/\partial h)$ . Woodworth et al. (2005) studied a seiche in Port Stanley harbour in the Falkland Islands which has a similar period (26 minutes) to that at Lerwick. Port Stanley harbour has a mean depth of about 6.8 m (averaged along the main axis of the harbour) and a tidal range of approximately 0.9 m. They demonstrated that, when one used values of seiche period from windows when the seiche amplitude was larger than its median value (so one could be confident that a real seiche was indeed present), then the variation of the period with changes in sea level (which are primarily due to the tide) implied an effective depth of 11 m, consistent given the simplicity of the method with the known depth of the harbour. Donn and Wolf (1972) provided another example of the expected dependence of seiche period on tidal height using data from Grindavik Harbour in Iceland.

A variant of the Woodworth et al. (2005) method has been applied to the present data set from Lerwick which has a tidal range similar to that at Port Stanley. A selection was made of the approximately 85% of measurements when seiche amplitude within a 6-hour window (Figure 3) was larger than 7 mm, and therefore when there was likely to be a meaningful estimate of seiche period. Then a regression of period in terms of the average measured sea level during the window yields a value for  $\partial T/\partial h$  of -0.82 min/metre (Figure 4a). If  $T$  is approximately 28 minutes, then that implies an effective depth  $H$  of 17 m, confirming that the seiche is generated in relatively shallow water, and not further offshore.

As in the cases of Balta Pier and Sella Ness discussed below, we found the effective depth obtained from the method to be somewhat dependent on the choice of threshold. However, the 85% requirement seemed optimal in order to reject measurements with no seiches, and yet retain enough measurements to make a statistically useful regression. See further below for discussion of the uncertainties with this method.

The temporary deployment at Lerwick North was made during December 2015 - January 2016 on the west side of the northern end of the north entrance of the harbour, approximately 3 km north of the Lerwick bubbler tide gauge (yellow dots in Figure 1c). It has useful data only for 2-25 December, and that was inevitably noisy owing to the measurement of instantaneous values of sea level every 3 minutes, rather than 3-minute averages. Figure 5 shows a modest enhancement in its spectrum at around 2 cph, similar to that at Lerwick, but peaking at a period of 24 instead of 28 min, when the transfer function magnitude is approximately 0.4 (i.e. Lerwick North has only 40% of the amplitude of Lerwick) and transfer function phase is approximately zero (i.e. the seiche is in phase at the two locations). Otherwise the spectrum is approximately flat for frequencies above 0.5 cph, indicating a quasi-white noise distribution that numerical simulations have shown is to be expected due to the low-frequency aliasing of a typical wave spectrum. We suspect that this larger background and the generally poorer quality of the record are responsible for the slightly different period of the peak at Lerwick North.

These findings can be interpreted by the harbour seiche being either a half- or quarter-wavelength resonance, with maximum amplitude at the head (north end) of the harbour. In both cases, given that the Lerwick bubbler gauge is located nearer to the node at the southern harbour mouth than at the anti-node at its head, the seiches at the head must be sizeable. Unfortunately, we do not have measurements there. Instead, Lerwick North was located at the northern end of the narrow north entrance. The only way to decide between the two possibilities is from knowledge of the currents associated with the seiche. In the case of a half-wavelength seiche, currents into the harbour from both the north and south directions will lead sea levels by approximately  $90^\circ$ . In the case of a quarter-wavelength resonance, the seiche would be associated primarily with currents from the southern entrance, leading sea levels by  $90^\circ$ , and with some northward leakage of seiche energy from the harbour into the north entrance. In both cases, seiche amplitude will decrease as one travels north up the northern entrance and the seiches observed at Lerwick and Lerwick North will be in phase, as observed. These alternative interpretations are discussed below using findings from our numerical model.

(ii) Balta Sound

Balta Sound is an inlet on the east coast of Unst, the northernmost of the main islands of Shetland. The Sound extends approximately 1.5 km northward from its entrance at the southern end of Balta Island, until a dog-leg, when it continues approximately 2.5 km westward up to its head. The township of Baltasound is located at approximately the centre of the north coast. A narrow (~250 m wide)

second entrance is at the northeast corner of the dog-leg, separating Balta Island from Unst (Figure 1d). The mean depth of the Sound, measured along its central axis, is approximately 12 m on the northward section from its main entrance up to the dog-leg, and then 8 m up to its head (NLS, 1924).

We deployed two sensors in Balta Sound: one at Baltasound pier ('Balta Pier'), where the previous measurements by Cartwright and Young (1974) were made, and one at a fish farm near to the mouth of the Sound that we call 'Balta Offshore' (yellow dots in Figure 1d). The latter was deployed on the sea bed by the operators of the farm at a depth of about 12 m.

The Balta Pier record shows a near-continuous seiche with a period of around 28 minutes, marginally longer than at Lerwick (Table 2). The seiche peak is narrower than that at Lerwick, while the overall shape of the power spectrum is similar to that described by Cartwright and Young (1974) (Supplementary Figure A(iii, BP)). An analysis similar to that described for Lerwick, and again with a 7 mm threshold that selects approximately 85% of measurements, yielded a value for  $\partial T/\partial h$  of -0.75 min/metre (Figure 4b). This implies an effective depth  $H$  of 19 m, which is larger than the known mean depth of Balta Sound, but suggests that the seiche is almost certainly generated in shallow waters in the area of the Sound itself rather than in deeper shelf waters. (Note that in this case, the 'h' used was necessarily the sea level equivalent of SSP, and not real sea level or water depth.)

The Balta Offshore record differs from that at Balta Pier in several respects. One is a short period of several days near the start of the record at days 278-281 (5-8 October) 2015, with high variability in the residuals (Figure 6a). This is almost certainly related to strong southeasterly winds at that time, and it is possible that there was occasional disturbance of the instrument. However, similar variability for those days is observed in the Balta Pier and Lerwick records although to a lesser extent. Otherwise, Balta Offshore contains the same 28-min seiche as Balta Pier but with a smaller amplitude.

Figure 7 shows power spectral density (PSD), magnitude-squared coherence and transfer function plots for Balta Pier and Balta Offshore. The two records have similar energy and are coherent at low frequencies but coherence drops for frequencies above 2 cph. The seiche peak at around 28 minutes, which is so clear in Balta Pier, is much reduced in Balta Offshore, with transfer function magnitude (Balta Offshore compared to Balta Pier) of about 0.2 and transfer function phase approximately zero.

These findings for the 28-min seiche can be interpreted as a quarter-wavelength resonance, with maximum amplitude (anti-node) at the head of the harbour above Balta Pier, and a node at the entrance nearer to Balta Offshore. This interpretation is also consistent with findings from the numerical model discussed below.

Cartwright and Young (1974) identified in their data from Balta Pier an unusually large 12<sup>th</sup> diurnal tidal component at a frequency of  $\sim 11.6$  cpd (i.e. M12). It was unusual in the sense that in most tide records one finds that the amplitudes of M4, M6 etc. decrease steadily with frequency until they reduce to noise level, whereas at Balta the 12<sup>th</sup> diurnal component was significantly larger than the 10<sup>th</sup> diurnal component.

We have confirmed that the large 12<sup>th</sup> diurnal component is also a feature of the new Balta Pier and Balta Offshore records, and the signals can be readily identified by eye in the spectra in the Supplementary Material. Harmonic analysis yields amplitudes for M12 of 1.1 and 1.3 mm respectively, whereas M10 is only 0.4 and 0.3 mm respectively, so we believe the Cartwright and Young (1974) observation to have been correct. They summed the total energy around the M12 spike in their spectrum and concluded that it contained energy of 10 mm<sup>2</sup> or amplitude of 3.2 mm, which is larger than our estimates from harmonic analysis. However, the 12<sup>th</sup> diurnal peak in our Supplementary Figure A(iii, BP) has a width that contains almost the same energy as that of Cartwright and Young

(1974). We believe their method must result in an over-estimate of the amplitude of M12 and that the peak must also contain other 12<sup>th</sup> diurnal terms such as 4MSN12, 5MS12 and 4M2S12. Nevertheless, our analysis and theirs clearly provide consistent conclusions as regards this anomalous 12<sup>th</sup> diurnal term. We return to discussion of this topic below.

(iii) Busta House

Busta House is located on the west coast of the Shetland mainland at the north end of Busta Voe which is an inland extension of an inlet from St. Magnus Bay called Swarbacks Minn. The sensor was deployed in a small harbour that emptied occasionally at extreme low tide, as shown by bottoming-out in short sections of the first half of the record. However, it is straightforward to identify and flag such sections of bottom-out and the record has proved to be acceptable. The short sections of zero residuals and zero standard deviation in Supplementary Figures A(i, BH) and A(ii, BH) respectively are artefacts of the bottoming out. Supplementary Figure A(iii, BH), which is spikier than the PSD plots from other stations, shows a broad peak of energy centred at a period of 48 minutes. There is also suggestion of some energy at shorter periods of 27, 22 and 16 minutes.

The whole Swarbacks Minn/Busta Voe inlet is about 11.5 km long, approximately 70 m deep at the entrance to Swarbacks Minn from St. Magnus Bay, shallowing to about 40 m in Busta Voe, although parts of the central axis of Swarbacks Minn exceed 100m depth. If one assumes a (rectangular, triangular) shape for the whole inlet (Rabinovich, 2009, Table 9.3), then one computes a period of 38 minutes, which is probably consistent with the 48 minutes observed.

There is no compelling evidence that the standard deviation of residuals varies as a function of the height of the tide. Nevertheless, Supplementary Figure A(ii, BH) provides some suggestion that the standard deviation is larger at springs than at neaps in the latter part of the record. It shows in blue the standard deviation of residuals in 2-hour windows, above which is shown in red the standard deviation of the measured SSP in the same windows (in practice, the standard deviation of the tide), offset and scaled for presentation purposes. Spring tides occur when the red curve is largest. However, on the other hand, this impression of a spring-neap component in the standard deviation of the residuals could be simply an accidental artefact of the short record.

(iv) Whalsay

This instrument was deployed at Symbister at the southwest corner of Whalsay Island, which lies off the northeast coast of the Shetland mainland, and faces the mainland inlet of Dury Voe. Supplementary Figure A(iii, W) has two main peaks at periods around 34 and 16 minutes.

(v) Toft

Toft is located on the south side of Yell Sound, the channel between the Shetland mainland and the island of Yell to its north. Supplementary Figure A(iii, T) suggests several peaks of which the most apparent are at 54 and 25 minutes. The energy of its residuals clearly depends upon the tide. As for Busta House, Supplementary Figure A(ii, T) shows in blue the standard deviation of residuals in 2-hour windows, above which is the standard deviation of the measured SSP in red. The spring-neap dependence of the tide is clearly reflected in the residuals.

(vi) Gutcher

Gutcher is located on the south side of Blue Mull Sound, the channel between the islands of Yell and Unst. Its main peak in Supplementary Figure A(iii, G) is around 42 minutes. Some association of the standard deviation of residuals with the tide, as shown for Busta House and Toft, might be seen

towards the end of the record when the standard deviation of residuals is relatively small, although it is not evident earlier.

We have not found an explanation for the 42-min peak. Most of it comes from a couple of individual events such as at the end of January 2016, as can be seen from the wavelet plot (Supplementary Figure A(iv, G)). Another unusual feature of the Gutchter spectrum (not shown) is that it is nearly monotonic between 4.5 cph (the upper limit of the spectrum in Supplementary Figure A(iii, G)) and 30 cph (the Nyquist frequency). This aspect is discussed further below with regard to numerical model findings.

(vii) Scalloway

Scalloway is situated at the head of small inlet called Scalloway Voe, which is a branch of a bay called The Deeps on the southwest coast of the Shetland mainland, at approximately the same latitude as Lerwick. It has several peaks in its spectrum (Supplementary Figure A(iii, S)), the largest having a period of 45 minutes, and with a series of higher-frequency peaks between 10-20 min.

(viii) Sella Ness

Sella Ness is located on the northwest of the Shetland mainland and is part of the Sullom Voe oil terminal complex. It is located on the east side of the north end of Sullom Voe, which is an inlet on the south side of Yell Sound.

Extensive measurements of currents were made in Yell Sound as part of the planning for the Sullom Voe terminal. Blackman et al. (1981) identified strong tidal and surge-related flows (some exceeding 2.5 m/sec) at locations in the Sound but no evidence was presented for currents associated with seiches. Dooley (1981) found tidal currents to be much weaker in Sullom Voe itself (approximately 7 cm/sec). In addition, he identified seiche-type events in the current meter data, with a period of approximately an hour and amplitudes of about 15 cm/sec, that were initiated apparently by sudden changes in wind direction. A similar period was observed in a short tide gauge record from Gravens Pier at the Sullom Voe site, where fluctuations in sea level exceeding 30 cm were found. Dooley (1981) concluded that the seiche period was not as well determined in the tide gauge data as in the current meter records because of the complicating presence of another seiche with a period of about 25 minutes.

The present Sella Ness tide gauge has provided a long, although somewhat gappy, record from which we have selected the most continuous section. It presents several strong peaks in its spectrum (Supplementary Figure A(iii, SN)) with periods of 81, 28 and 15 minutes. We suspect that the first two of these correspond to those observed by Dooley (1981). He noted that a quarter-wavelength resonance of Sullom Voe, given its axial length of 13 km and average depth of 25 m, would have a period of about an hour. The fact that a similar 81-min peak is not observed in the data from Toft confirms that the seiche is more local to Sullom Voe rather than distributed more widely in Yell Sound.

This conclusion was confirmed by once again testing how period changes with depth, although initially we considered the method might not work so well for a broader and lower-frequency seiche peak. Seiche amplitudes are much larger in this case than at Lerwick or Balta Pier, and a higher threshold of 15 mm was required in order to retain approximately 85% of measurements. Figure 4(c) provides a value for  $\partial T/\partial h$  of -1.78 min/metre, which corresponds to an effective depth of 23 m. The numerical model discussed below also suggests that the seiche is primarily a resonance of Sullom Voe rather than of Yell Sound.

(ix) Out Skerries



Out Skerries is a group of small islands approximately 10 km to the east of the Shetland mainland. The gauge was deployed at the ferry terminal on the island of Bruray. It was selected, together with Fair Isle, as an off-shore location which might exhibit contrasting seiche behaviour compared to that at mainland locations. Supplementary Figure A(iii, OS) shows no strong peaks, apart from perhaps a suggestion of a minor enhancement at 43 minutes.

(x) Fair Isle

Fair Isle is small island between the Shetland and Orkney islands, approximately 40 km south of the southern tip of the Shetland mainland (Figure 1a). Our gauge was deployed at the north end of the island in a small harbour near to the Fair Isle Bird Observatory. Its record was short and the gauge was evidently disturbed on several occasions. The end of the record exhibited high variability that we do not believe is real, and so it has been truncated to end at the same time as the Out Skerries record. There are no strong peaks in its spectrum (Supplementary Figure A(iii,FI)).

### 3.3 Features in common between sites

Figure 6(a-b) presents the time series of residuals for the two periods for which we have measurements from several sites simultaneously: September-December 2015 and December 2015-April 2016. The residuals are larger at some sites than others, as shown by the standard deviations of each record in Table 2. Those on the west coast (Busta House, Sella Ness and Scalloway) exhibit larger variability in the residuals than those on the east coast, with the exception of Lerwick North which we have mentioned is probably noisier for instrumental reasons.

Figure 6(c) shows the residuals from measurements at the two outer islands (Out Skerries and Fair Isle) during the summer months April-August 2016, together with Lerwick for comparison. The two islands have much lower variability in the residuals than for stations in Figure 6(a,b), which will be partly due to the data being collected in summer, Lerwick also having a lower standard deviation in this period than in Figure 6(a,b) (although discussion of the July 2015 event below demonstrates that summer is never free of seiches). This lower variability is consistent with that observed over 3 summer months at another offshore island (Foula Isle, approximately 30km from the SW coast of mainland Shetland) as discussed by Cartwright and Young (1974). (The extensive set of tidal measurements in this area by David Cartwright, which included those at Foula discussed in Cartwright and Young (1974), was described by Cartwright et al., 1980).

Figure 6 (a-c) shows that, in general, any higher variability in the residuals tends to be energised at the same time at each place, whether that is in the south or north of Shetland, on the west or east coasts, or on the outer islands (Figure 6 (c)). It has been shown that the high-frequency variations at each site are different in magnitude, and have different spectral components. Nevertheless, common sense suggests that they must be energised in a similar way (e.g. by the same synoptic storms).

Table 2 shows that there are peak frequencies that are approximately the same at more than one site. For example, a period of approximately half an hour occurs at Lerwick, Lerwick North, Balta Pier, Balta Offshore, Toft, Gutcher, Whalsay and Sella Ness. A period of about  $\frac{3}{4}$  hour is found at Busta House and Scalloway. Several sites have peaks at around 15-20 minutes. It is possible that several of these signals have a spatial scale that means they are genuinely common to more than one site, any small differences between peak frequencies being due to differences in the background continuum of variability at each location.

## 4. Larger seiche events at Lerwick

#### 4.1 Seiche events on 2 July 2015 and 28 May 2008

Sibley et al. (2016) described the intense thunderstorm activity that moved from the north of England into Scotland on the evening of 1 July 2015. This had been one of the hottest days of the year. Unusual high-frequency oscillations in sea level were detected at the same time along the east coast of Scotland, including at Stonehaven where violent water motions in the harbour caused damage and injury, and at the Aberdeen tide gauge where oscillations persisted into the first part of the next day. Evidence of surface air pressure fluctuations of several hPa were obtained from a number of observation sites in northeast England, east Scotland and the North Sea, which correlated with the passage of the storm system. The general interpretation was of a series of events akin to meteotsunamis (Šepić et al., 2015; Pugh and Woodworth, 2014; Vilibić et al., 2016). The weather and sea levels in Shetland were not discussed.

In fact, Shetland had similar experiences. The *Shetland Times* reported intense thunderstorms in the early hours of 2 July, mostly in the west of the mainland (near to Busta House) that resulted in power outages. At Lerwick there was a small increase of surface air pressure of about 1.5 hPa at 4.50 am (GMT) followed by an abrupt fall of about 5 hPa by 5.25 am, similar to the pressure jumps that were observed elsewhere (Figure 8). At the same time there was a change in wind direction, while wind speed and maximum wind gust had increased about half an hour before (Supplementary Figures B(b,d)). (These 1-min values are averages of 240 ¼-second spot measurements. Maximum gust, following World Meteorological Organization convention, is calculated as the maximum speed averaged over a 3 second period within the minute.)

This rapid air pressure oscillation was most likely responsible for the residuals in the Lerwick sea level record of the order of 0.5 m at about the same time (Figure 9). It will be shown below that these are some of the largest on record. Fluctuations had already started in the evening of the 1 July, and were large again at the end of 2 July (when Figure 8 shows there were other pressure fluctuations), and continued for several days afterwards, suggesting a series of atmospheric disturbances. Meanwhile, it is known that a survey vessel was almost run aground in Lerwick harbour by unusual currents that were possibly due to the seiche (private communication, Lerwick Port Authority).

Sibley et al. (2016) also reported on another event, on 28 May 2008, that they claimed had a similar origin. They made use of publicly-available 15-min average sea level data from Lerwick, indicating a 14 cm fluctuation over an hour just before midday, which continued for a further day or so. Their presentation of this event was not as convincing as it could have been, as averaging over 15 minutes will dampen considerably any high-frequency seiche signals.

After the Sumatra tsunami of 2004, NOC installed so-called 'tsunami gauges' at several of its sites, one of which was Lerwick. These were experimental installations that used differential strain-gauge pressure sensors fixed below low tide. They were maintained for some years on a 'best efforts' basis, primarily thanks to the initiative of Mr. Les Bradley, and they were to be replaced eventually in 2015 by high-rate sampling of the bubbler gauge. NOC has such 'tsunami data' for 2008, acquired at 1 Hz. These data are shown in Figure 10, demonstrating that sea level fluctuated just before midday on 28 May by about 50 rather than 14 cm, and that significant fluctuations reoccurred around midnight on 29/30 May. Therefore, there is perhaps more similarity between the events of 2 July 2015 and 28 May 2008 than Sibley et al. (2016) suggested.

#### 4.2 Lerwick 15-minute data

As we have shown, 15-min data is inadequate for a proper description of the individual seiche events at Lerwick. Those events tend to be dominated by variability with a period around 28 minutes which

is near the Nyquist period for the sampling. However, it is still possible to use these data to determine how often, and at what times of the year, that large-amplitude seiche events occur.

The Lerwick tide gauge records available from BODC commence in 1959. The earlier data are in the form of hourly values which are not useful for the present study. There was an improvement to the provision of 15-min average values in January 1993 and this remains the situation today.

Each month BODC performs a quality control (QC) of the 15-min tide gauge data from the national network including Lerwick. Part of that procedure involves a separation of the data into 'tide' and 'non-tidal residual (NTR)' components. The former is based on the best available set of harmonic constants available for the port in question at the time that the QC is performed, and the latter is the difference between the measurements and the tide. The NTR values are not to be confused with the 'residuals' as we have defined them above, obtained from 1-min data.

The best sets of harmonic constants are updated occasionally, and those updates will slightly affect the calculated 'tide' and NTR time series. Nevertheless, the procedure should have been uniform enough over time for our purposes, as the best constants for a port such as Lerwick will not change significantly from year to year. All NTR values together with the 15-min measurements can be obtained from the BODC web site. We have used NTR values from January 1993 - September 2016 in a method as follows.

In principle, the NTR values should contain only those signals originating from non-tidal processes such as seiches, storm surges and changes in mean sea level. We compute the standard deviation of NTR values (SD-NTR) within moving windows; experimentation showed windows containing 9 15-min values to be optimum. (A trend is removed from the 9 values prior to computing the standard deviation.) The numerical value of SD-NTR is, of course, much smaller than the sometimes  $\pm 0.5$  m observed for the residuals in Figure 9. However, it is used here to indicate which times that high variability occurs, rather than to provide a precise quantitative value of that variability.

As an example, Figure 11(a) shows SD-NTR during the July 2015 event mentioned above. It can be seen that large values of over 100 mm are obtained from the 15-min NTR values at the same times as large residuals are obtained from the 1-min values in Figure 9.

We can then progress to plotting SD-NTR for all available data since 1993. Figure 11(b) shows the SD-NTR values for an example complete year (2015), showing high values in January and December as well as in early July. The method also picks out the May 2008 event discussed by Sibley et al. (2016) (Figure 11c). Once again it can be seen that there were several large events in that year.

There are large gaps in some years of data. Nevertheless, there are enough complete or near-complete years from which to determine the times of SD-NTR above some threshold, and so obtain a climatology of large events. Table 3 gives the number of times that there is a window with an SD-NTR of 15-min values above a threshold of either 30 or 60 mm, for years that are at least 85% complete. It also gives the numbers in winter and summer separately (defined as the first and last, and the middle two, quarters of the year respectively) and the fraction in winter. Both thresholds suggest that 1993 had the largest amount of seiche activity, followed by 2015 for the lower threshold, or 1999 for the higher. In 13 and 12 years for the lower and higher thresholds respectively, out of 16 near-complete years of data in all, seiche activity occurs more in winter than summer.

The July 2015 event can be shown to have been very unusual by setting the threshold to a high value of 120 mm (Figure 11b). The May 2008 event is not selected in this way, having high SD-NTR values but somewhat below that high threshold (Figure 11c). Similarly, there are high SD-NTR values of

approximately 60 mm on 25 December 1999, although again below the high threshold. This was the day with the lowest air pressure (944.4 hPa) ever recorded at Lerwick (Burt, 2007). In fact, there is only one other example in the data set of SD-NTR above the high threshold, on 4 September 1996, but in this case the NTR values analysed include several that are interpolations by BODC rather than genuine measurements. Although this was another period of very warm weather and high air pressure, this example can probably be rejected as a meteotsunami candidate similar to 1-2 July 2015 given that the weather record from Lerwick provides no evidence for pressure jumps or thunderstorm activity at this time.

#### 4.3 Forcings for most of the Lerwick seiches

We have shown that the main seiche period at Lerwick is about 28 minutes. A first point to make is that there is no particular meteorological forcing with this period. Figure 12(a) shows the lower frequency part of a power spectrum of surface air pressure at Lerwick computed from 2 years of 1-min values, indicating a line at S2 with a period of 12 hours (0.0833 cph). This spectral line is expected, as an S2 (and sometimes S1) air tide is found in many barometer records around the world (Pugh and Woodworth, 2014). The existence of this line suggests that the Lerwick air pressure data are reliable. Figure 12(b) shows the higher frequency part of the spectrum; no peaks are evident at periods similar to those of the seiches in Table 2.

If we leave aside meteotsunamis as an important reason for seiche activity, events such as those in July 2015 and May 2008 discussed above being very unusual, then strong winds are the obvious primary candidate, particularly in winter. The top row of Figure 13 (a) shows the amplitude of 28-min seiches at Lerwick during 2015, as given previously in Figure 3, but here divided by the standard deviation of the time series, so as to enable ready comparison to the meteorological information beneath. (Note that the large seiche amplitudes around 2 July 2015 exceed the upper plot limits.) The second row shows 1-min values of surface air pressure, also scaled by its standard deviation, the third row gives wind speed similarly scaled. (The maximum wind gust time series is very similar to that of wind speed and is not shown.)

The first thing is to note that the large 2 July event was clearly anomalous. Otherwise, it can be seen that there was greater seiche activity towards the end of the year, which was a period of high wind speeds, that corresponds also to findings of higher seiche activity at that time from the SD-NTR analysis (Figure 11b). Wind direction in that period was generally from the southwest, as it tends to be normally (cf. Supplementary Figure D(v)). We did not find a stronger association of seiches with winds during the year by separating winds into their along- and cross-shore components.

On the other hand, the smaller peaks in 28-min seiche amplitude during the summer months in Figure 13(a) are associated more with lows in air pressure rather than by stronger winds. The red dashes indicate some of the events for which inspection of Met Office synoptic charts confirms the passage of depressions at these times.

Figure 13(b) shows the corresponding information for the first part of 2016. As shown in Figure 3, the end of January 2016 experienced high seiche activity, and values of amplitude in Figure 13(b) exceed the upper plot limits. This was once again a period of exceptionally strong winds. There was another event with strong winds and low air pressures in March. Otherwise, there were several other periods of seiche activity through the spring that are primarily associated with depressions, as in summer 2015.

Cartwright and Young (1974) used measurements at Lerwick and Baltasound in the summer months of May-August 1972. They decided that their larger seiches were not produced 'by mere force of wind'

but the likely rapid passage of frontal systems with associated sudden changes in wind direction. This suggestion seems consistent with our findings, at least for the summer seiches (Figure 13). A similar association of seiches with the passage of low pressure systems in the North Sea region was observed in Rotterdam harbour by de Jong et al. (2003).

It is also of interest to consider whether seiches occur at different states of the tide. For example, they could be energised by tidal currents which are usually largest at mid-tide. On the other hand, one would imagine that seiches generated by storms would occur throughout the tidal cycle.

Figure 14(a) is made by first filtering the Lerwick residuals so as to select the '28-min band' of variability in their time series (in this case defining the band as 1-3 cph, see the Supplementary Material Set C for use of a narrower band 1.7-2.4 cph). Then the standard deviation of the filtered residuals is computed within moving 2-hour windows. Finally, the median standard deviation is calculated as a function of the height of the tide (shown in blue). In order to remove daily and longer-term changes in the mean level, and so have a better representation of tide height and therefore currents, the height of the tide is defined relative to a level averaged over  $\pm 12$  hours. This procedure has a further advantage in allowing sea level and SSP time series to be analysed the same way.

There is a suggestion of lower values of median standard deviation at high and low tide, and more clearly in the 90-percentile standard deviation (i.e. when the largest seiche activity occurs, shown in red). No evidence of significant tidal dependence can be seen in the 10-percentile standard deviation (i.e. when seiche amplitudes are low, also in red). The percentile values for the very lowest and highest tide levels in each of these distributions are necessarily statistically less reliable.

Figure 14(b) shows the median curve for the whole record once again (in blue) and also the median standard deviations for tidal range above (red) and below (green) the mean tidal range (i.e. periods of spring and neap tides respectively). The red curves inevitably span a greater range of tide height than the green ones. There is little evidence for differences between the three curves within their common span of tidal height, but once again there is some evidence for lower standard deviation near the tidal turning points, when tidal currents will be lowest.

The Supplementary Material (Set C) contains the corresponding figures for several other stations and for the appropriate filtering in each case where there are clear peaks in the spectra. These include Balta Pier (Supplementary Figure C(iii)) where there is little evidence in these for a dependence of standard deviation with either the height of the tide or with spring-neap variation in the tide. On the other hand, at Toft, for which no filtering of the residuals was made (Supplementary Figure C(iv)), larger seiches occur preferentially towards high tide, and have almost double the magnitude of standard deviations at springs than at neaps. Toft is located in an area of strong tidal currents through Yell Sound (Halliday, 2011). At Scalloway (Supplementary Figure C(v)), there is also no variation with tidal height but standard deviations are slightly larger at springs. A similar conclusion applies to Sella Ness data using either a 60-120 or 25-35 min filter, so selecting the two main seiche peaks (Supplementary Figures C(vi,vii)). Scalloway and Sella Ness can, therefore, be interpreted as seiches occurring more strongly at springs and, when they occur, they take place throughout the tidal cycle. At Gutcher, where there are strong currents through Blue Mull Sound, there are larger seiches towards high tide but no significant spring-neap variation (Supplementary Figure C(viii)). Finally, Whalsay presents a more complicated example, with largest 90-percentile standard deviations at mid-tide, but little dependence on the tide for the median and 10-percentile standard deviations, and approximately the same standard deviations at springs and neaps (Supplementary Figure C(ix)).

Consequently, it can be seen that the tide plays a role in generating, or modulating, seiche activity at some locations, although Figure 14 and figures in the Supplementary Material Set C suggest that, with the possible exception of locations such as Toft, it is not the dominant forcing.

#### 5. A numerical model of Shetland seiches

A 2-dimensional numerical model was constructed using the MIKE 21 FM (flexible mesh) scheme of the Danish Hydraulic Institute (DHI, 2010). The region covered was approximately 44-66°N and 17.5°W to the European coast. Tidal forcing at the open boundary was provided by the TPX07.2 model which is an updated version of that described by Egbert et al. (1994), while wind and air pressure forcings were computed from spatial interpolations of hourly ERA5 fields (C3S, 2017). (Earlier model experiments were undertaken using the coarser 3-hourly ERA-Interim fields, Dee et al., 2011).

Model bathymetry was taken from the General Bathymetric Chart of the Ocean (GEBCO) (<https://www.gebco.net>, Weatherall et al., 2015) at 0.5 minute resolution, apart from that around the Shetland Islands (approximately 0.65-1.79°W, 59.72-60.93°N) which was obtained from the European Marine Observation and Data Network (EMODnet) portal (<http://www.emodnet-bathymetry.eu>) at 1/8 minute resolution (approximately 250 m east-west and 450 m north-south). Additional bathymetric information for Lerwick and Balta Sound harbours was added from Admiralty Charts from the National Library of Scotland (NLS, 1924, 1927). Mean depths were defined by adding 2 metres to EMODnet and NLS values, which are stated to be relative to Lowest Astronomical Tide and Mean Low Water Springs respectively. The resulting finite-element grid containing 238035 grid points was based on the above information on water depth and coastal topography, with a fine grid (~50-200 m) used for coastal waters and a coarser grid for deeper waters. Sea levels and U and V components of current at each grid point were output by the model every minute.

The bathymetry we have used for the two harbours is coarse and can undoubtedly be improved. Nevertheless, it was considered adequate for a qualitative model study. However, the bathymetry for other locations around Shetland relies entirely on EMODnet, which is known to be completely inadequate very close to the coast. There was no other practical choice of bathymetry available to us. Consequently, the findings from the model mentioned below have to be considered with that in mind.

It is important to clarify that it was not possible to use the model to its fullest extent for comparison to the tide gauge data, given its coarse wind forcing and bathymetry. Consequently, it cannot be expected to reproduce many of the detailed features of individual seiche events. Instead, we have used the model only as a means of introducing energy into the model grid in order to determine the main spatial patterns of high-frequency sea level variability, and their associated periods, that are a consequence of resonance due to coastline shape and bathymetry.

We made use of 2 model data sets, each one spanning approximately 7 days (1-7 January and 1-7 July 2015) with the first day in each case used for model spin-up. These two short periods were chosen initially in order to force the model with very different wind fields, resulting in greater high-frequency sea level variability on the west and east coasts respectively (Supplementary Figures D(i,ii)). As shown in Supplementary Figures D(iii,iv), wind direction had a very different statistical distribution in these two short periods. During the January run, winds spanned directions from the south to the northwest, while during the July run they were mostly either from the east, south or west. It was not possible to run the model for the entire measurement period in 2015-2016. Consequently, any conclusions regarding the dependence of seiches on winds during most of our measurements must be made by considering findings from these two runs in combination, noting that wind directions during the measurements covered a different range to those during both of the short runs, spanning directions from west to east and most frequently from the southwest (Supplementary Figure D(v)). (In addition,

we know from Figure 6 that in reality high-frequency sea level variability occurs at approximately the same times (i.e. within days) on the east and west coasts (with larger variability for the latter), so in practice one never has a simple situation of extended periods of westerly or easterly wind forcing.)

Supplementary Figure D(vi) shows the spectra of 1-minute sea levels from the model for Lerwick and Balta Pier from the July run, and Scalloway and Sella Ness from the January run, at times when the east and west coasts respectively tended to be energised preferentially. A broad peak at approximately 2 cph can be seen for Lerwick and a narrower one for Balta Pier, qualitatively consistent with the measurements. Scalloway has a peak at  $\sim 1.3$  cph and Sella Ness at  $\sim 0.7$  cph also consistent with the main frequencies in the observations shown in Table 2. Consequently, while the model is not perfect (especially with regard to its coastal bathymetry), it does reproduce qualitatively many of the features in the data. (We have already shown in Figure 12 that the periods of such resonances are not related to meteorological periodicities.)

The main temporal and spatial modes in the model, indicating which parts of the coast resonate at particular frequencies, are demonstrated in the Supplementary Material for the January and July 2015 runs (Supplementary Figures D(vii-ix) and (x-xii) respectively). They are shown in terms of the variance found at points in the grid within the broad frequency bands 0.5-1.5, 1.5-2.5 and  $>2.5$  cph.

The first band (0.5-1.5 cph) with periods centred approximately on 1 hour, shown in Supplementary Figures D(vii and x), corresponds to variability primarily in Sullom Voe, which contains Sella Ness, and in the inlets of Yell Sound to its east. The January run also shows energy at this frequency in the bay called The Deeps on the southwest coast of Shetland which contains Scalloway, and in St. Magnus Bay on the west coast of the Shetland mainland and its inlet called Swarbacks Minn which contains Busta House. This result is consistent with our measurements of the main seiches at these locations, discussed above.

The second band (1.5-2.5 cph) with periods centred on about half an hour has for the July run (Supplementary Figure D(xi)) localised areas of high variance in Burra Firth on the north coast of Unst, Balta Sound, Dury Voe and Lerwick Harbour on the east coast (each discussed below) and several other east coast inlets. This figure demonstrates, at face value at least given the bathymetry concerns mentioned above, how the half-hour seiches are confined to particular inlets. For the January run (Supplementary Figure D(viii)) inlets in The Deeps in the southwest are energised preferentially, although Burra Firth, Dury Voe and other inlets are also represented.

The third band spanning frequencies above 2.5 cph picks out in the July run (Supplementary Figure D(xii)) many of the locations in the 1.5-2.5 cph band (i.e. Balta Sound, Dury Sound and Lerwick Harbour) as well as Blue Mull Sound, between the islands of Yell and Unst, and other localised areas. For the January run (Supplementary Figure D(ix)), Blue Mull Sound is again represented but otherwise only some small inlets in the south and west of the Shetland mainland, consistent with higher frequencies being associated with shorter spatial scales.

These three bands are each rather broad and in discussion of particular stations it is desirable to adapt them slightly. For example, as discussed further in the next section, the 28-min seiches at Lerwick and Balta Pier are reproduced adequately when model time series are filtered to isolate a band spanning 25-35 minutes (1.7-2.4 cph), which is a band that can be taken as applying to both locations in the real measurements (see Supplementary Material Set C). In that case, one obtains the maps shown in Figure 16 and Supplementary Figure D(xiv). Of course, the similar frequencies in real and model data are somewhat fortuitous given the coarseness of the model bathymetry. Nevertheless, the seiches are clearly suggested to be localised resonances. In addition, in the case of Lerwick, Figure 16 shows the largest model amplitudes at the head of the harbour, but not to any extent in the narrower northern

entrance, consistent with our findings for Lerwick North (although the limitations of the spatial resolution of the model grid have to be kept in mind in this area). Other examples of local resonance are at Burra Firth (Supplementary Figure D(xiv)) and Dury Voe (Supplementary Figure D(xv)) that are discussed below.

A further example concerns the main seiche at Sella Ness. Supplementary Figure D(xvi) shows that when model time series are filtered in the band 0.5-1.0 cph, thereby focusing on the '81-min seiche', then the seiche is contained within Sullom Voe itself, rather than in Yell Sound or over a wider area, consistent with the measurements discussed above. The second seiche identified in the Sella Ness spectrum, with a period of about 28 minutes (Supplementary Figure A(iii, SN)), could well be an even more localised resonance of Garths Voe, the bay which contains the oil terminal at the northeastern end of Sullom Voe. A final example concerns band-passed sea level variability in the model at the highest frequencies (i.e. for periods less than 25 minutes). One area of interest identified using this band is Blue Mull Sound (Supplementary Figure D(xvii)), for which inspection of model currents and elevations for both the January and July model runs suggests a half-wavelength resonance, with sea level variations in-phase throughout the Sound and currents into the Sound from both directions leading sea levels. If this modelling aspect is correct, it would be an explanation for the monotonic spectrum for frequencies above 4.5 cph in the Gutcher spectrum mentioned above.

In summary, the examples show that there are many aspects of similarity between the model and the measurements regarding the locations, periods and spatial extents of the main seiches.

## 6. Cartwright and Young (1974) revisited

### (i) Origin of the Lerwick and Balta seiches

One motivation for the present study was to revisit the findings of Cartwright and Young (1974) from measurements made during May-August 1972. They studied the broad peaks in the sea level spectra at a period of approximately 28 minutes at Lerwick and Baltasound (their Figure 4). Figure 15 provides our own comparisons of the two sites. Figure 15(a) shows that the width of the '28-min' peak is broader at Lerwick, as Cartwright and Young (1974) demonstrated. In addition, they observed that, even though packets of variability occur at about the same times (Figure 6a), there is little coherence between them at the seiche frequency (Figure 15b).

Cartwright and Young (1974) discounted the possibility of the seiches being due to local resonances, by arguing that the typical depth of the coastal sea was about 50 m. Therefore, a period of about 28 minutes would imply a wavelength of 38 km, or half-wavelength of about 20 km. They said that this "precludes extremely local motions which might be set up in the narrow sound of Bressay and Balta where the tide gauges were". However, this argument is incorrect in two respects: (1) that the depths of the two sounds in question are much less than 50 m, and (2) that any local resonances could be quarter-wavelength ones, instead of full or half-wavelength resonances.

In fact, in our ocean model, the energy in this 28-min band (1.7-2.4 cph) at both Lerwick and Balta is associated primarily with local resonance. Figure 16 (a) shows the variance in sea level and the U and V components of current at Lerwick. Cross-spectral analysis shows that flows into the harbour from both the south and north entrances (primarily the V components of the flows) lead sea level variations in the harbour by 90°, as expected for a half-wavelength resonance (although an asymmetric one in this case). At Balta Sound, shown in Figure 16(b), there is flow into the harbour from only one direction (primarily via the U component); the inward flow leads sea level at the head of the Sound by 90°, indicating a quarter-wavelength resonance. Of course, sets of current meter measurements would be required to confirm whether these model findings are correct at each location.



Quarter-wavelength resonance for this 28-min band is found in the model even more strongly at Burra Firth on the north coast of Unst, close to the Muckle Flugga lighthouse (Figure 16b). Unfortunately, we do not have measurements at this location. In addition, there is an apparent quarter-wavelength resonance in a similar frequency band in an inlet called Dury Voe on the northeast coast of the Shetland mainland, opposite the island of Whalsay (Figure 16c). Again, these model findings will depend on the reliability of bathymetric information in these areas (EMODnet in this case).

Having discounted the possibility of local resonances, Cartwright and Young (1974) were encouraged by the similarity of the Lerwick and Baltasound spectra to propose a model involving coherent resonance of the entire east-facing Shetland shelf. This led to a description of edge waves which can travel both north and south, that combine into standing waves along the coast, with current nodes roughly 25 km apart and with largest sea level amplitudes in the central part of the east coast, at approximately the latitude of Whalsay.

However, there are several aspects of the new data set which argue against this interpretation. One is that, as Cartwright and Young (1974) noted, their model would impose a fixed phase relationship between the Lerwick and Baltasound 28-minute seiches, whereas in fact there is none (Figure 15). A second is that the 28-min seiche is considerably reduced in the Balta Offshore data, compared to that at Balta Pier (Figure 7), while any genuine shelf process would have been expected to contribute equally at both Balta stations. The third is that, even though Whalsay has a peak in its spectrum similar to that at Lerwick and Balta Pier (Supplementary Figure A(ii,W)), but at a slightly lower frequency, its amplitude is less than half that at the other two locations, which contradicts the Cartwright and Young (1974) suggestion. Instead, we suspect that the small Whalsay peak could be due to Symbister (where the gauge was located) being in the tail of a possible quarter-wavelength resonance of Dury Voe (Figure 16c). The absence of a strong peak at Whalsay with a period around half an hour is supported by the absence of one also at Toft, which is less than 20 km distant. The absence of one also at Out Skerries, at a similar latitude (Figure 1b), is not conclusive either way as the edge waves proposed by Cartwright and Young (1974) would have amplitudes that reduce exponentially with distance from the mainland coast. Cartwright and Young (1974) stated that “to account for the facts more fully would require consideration of higher wave modes ... and a more sophisticated mathematical structure”, which we suggest, given the evidence of our new data set, would not be worthwhile pursuing.

Cartwright and Young (1974) deserve credit, however, in recognising that seiches are best studied using information from nearby stations in combination, and Woodworth (2017) has recently shown that data from a regional network is even more useful. However, the published literature on seiches is almost entirely comprised of studies of individual stations. The only historical study of seiches known to us which has some similarity to that of Cartwright and Young (1974) is that of Inman et al. (1962), who investigated seiches at two locations on the Argentine shelf 120 km apart (compared to 70 km between Lerwick and Balta Sound). The Inman et al. (1962) findings were similar to those of Cartwright and Young (1974), concluding that seiches at each location occurred at about the same time, associated with the passage of sharp meteorological fronts, but with no coherence between them.

In summary, the best explanation for the half-hour seiches at Lerwick, Balta and Whalsay is a set of local resonances with slightly different periods that are determined by the topography of each inlet. The larger events would be energised by long waves impinging on the inlets originating from wind setup and swell produced by the same storms (Figure 6). And at least two of the largest known events at Lerwick appear to be associated with the long-waves arising from meteotsunamis (Section 4.1). To that extent, there could well be common long-wave forcing of the seiches at different locations, if not exactly in the way proposed by Cartwright and Young (1974).

No further insight was obtained from either our recent measurements or from our model by means of which the Cartwright and Young (1974) model could be tested. In principle, something more could be learned from coastal current meter measurements. A number of acoustic Doppler current meter records from around the Shetland coast were made available to us by the Scottish Environment Protection Agency (SEPA). These data were collected as part of the assessment requirements of fish farm licensing. Most of the records span two weeks to a month, and have 10 or 15 minute sampling. They show clearly the ebb and flow of tidal currents. However, the tidal signals and general noise dominate over any evidence for seiches in the data. Wolf et al. (2015) identified a few other data sets of currents around Shetland, acquired since 2000. However, it is uncertain whether they are freely available and have suitable temporal sampling for seiches.

(ii) Tidal ringing

Cartwright and Young (1974) suggested that the anomalous M12 component in their Balta Sound record arose from a process they called ‘tidal ringing’. They observed that anomalous M12 (i.e. M12 amplitude larger than M10) had also been observed in bottom pressure recorder (BPR) data from the shelf edge to the west and north of Unst, whereas M12 was more conventionally smaller than M10 at the Lerwick and Foula coastal tide gauges in southern Shetland, and in BPR data from southwest of Shetland and in the North Sea to the east of Unst. Shelf resonance would occur with a frequency given (neglecting rotational effects) by  $\sqrt{gh}/4b$  where  $h$  and  $b$  are shelf depth and width respectively and  $g$  is acceleration due to gravity. The authors developed this theory in some detail, and the implication seems to have been that energy from the northwestern shelf would have propagated around the east coast of Unst to be observed in Balta Sound.

Most of the records used by Cartwright and Young (1974) spanned only a few months, while their BPR records were even shorter at about one month. Consequently, we can make several important contributions to this discussion using our more copious recent coastal data set.

Supplementary Figure E1 shows the amplitudes of M4 to M12 for the seven northern stations in Figure 1(b) and also Lerwick for comparison (calculated using harmonic analysis, even harmonics only). For example, those from Lerwick (green dots) or Out Skerries (blue diamonds) have similar amplitudes for M4 and M6 and then amplitudes decrease approximately exponentially with degree, unlike the two from Balta Sound (red dots) for which there is the anomalously large 12<sup>th</sup> diurnal component. The similarity of the two Balta Sound curves is reassuring, as is the similarity of the three from the area of Yell Sound (Sella Ness, black diamonds; Whalsay, black dots; Toft, black asterisks). Gutcher (blue dots) is the nearest of our other stations to Balta Sound; its amplitudes also decrease approximately exponentially with degree.

In support of Cartwright and Young (1974), we can confirm their finding that M12 is anomalously larger than M10 at Balta Sound, both at Balta Pier (where their data were also obtained) and at Balta Offshore. However, M12 is smaller than M10 at all of our other stations (with the exception of Busta House which we did not use given its noisy spectrum owing to the bottoming-out mentioned above, see Supplementary Figure A(iii, BH)). These findings indicate that Balta is indeed special in some way.

However, in contradiction to Cartwright and Young (1974), we can point to Gutcher, located only 13 km from Balta Sound. Its record would also surely have included any anomalous M12 from the northwest shelf if their theory was correct. M10 at Gutcher has an amplitude of 2.1 mm whereas that of M12 is 0.4 mm. This seems to us to be sufficient to invalidate the northwest shelf tidal ringing theory. In addition, although less reliably, we found M12 at Fair Isle, located in the south of our area

(Figure 1) to have almost the same amplitude as M10 (both about 2.2 mm), at least for the first half of an admittedly poorer-quality record. Fair Isle is a long way from the northwest shelf.

## 7. Discussion and Conclusions

The acquisition of a set of 12 tide gauge records from Shetland has enabled us to show that the coastal waters around Shetland have a rich collection of seiches, with most locations having one or more seiche peaks in its spectrum. We have attempted to understand as far as possible why these oscillations occur and if they result from the same forcing. We have observed that, whichever inlet they occur in and whatever their period, the seiches are generated at approximately the same times by the same meteorological events, with seiches on the west coast being more energetic than on the east coast (Figure 6). Furthermore, at locations where two or more seiche modes are observed in the same spectrum, the wavelet plots demonstrate that the individual modes tend to be energised at the same times. At some locations (e.g. Toft), the tide also evidently has a role in modulating the seiches. This is perhaps to be expected given that the tide has been found to affect the forcing of seiches at other locations (e.g. Ichiye and Dowling, 1960; Golmen et al., 1994; Park et al., 2015, 2016).

Identification of a peak in a power spectrum such as that for Lerwick (Figure 2a) can sometimes be taken as evidence for a seiche in a harbour or inlet, when its period is consistent with its known dimensions. However, such an interpretation is not always conclusive. For example, if an inlet was about 3 km long and 5 m deep, and the neighbouring shelf was approximately 9 km wide and 40 m deep, then the peak with period about half an hour could as easily be due to quarter-wavelength resonance of either one or both. Therefore, it helps to have measurements from more than one site in the area, such as we have from Lerwick and Balta Sound, in order to investigate how the amplitude and phase of the seiche vary spatially. Data from these two sites suggest that they are local resonances of their respective sounds with the 20-30 minute periods one would compute readily from a rough idea of their lengths and depths (Rabinovich, 2009).

It is also useful to have a large tidal range so one can study how seiche periods change with water depth using a method such as in Section 3.2. That method seems to work well for harbours with clear bounds such as Port Stanley, which is essentially an enclosed one-dimensional body of water where the seiche is a half-wavelength resonance as in a lake, or Grindavik (Figure 2 of Donn and Wolf, 1972). It is more problematical when one has an inlet with an open mouth. In that case, the node can change its position slightly during the tidal cycle, meaning the period would depend also on a varying effective harbour length (and possibly width) as well as its depth. This might explain why in the cases of Lerwick and Balta Pier discussed above, a larger effective depth was obtained than might have been expected, although at Sella Ness, which is a much longer inlet, approximately the right value was obtained. The method also selects periods that are slightly smaller than that of the seiche peak at some locations (e.g. Lerwick, Figure 4a) but are as anticipated at others (e.g. Balta Pier, Figure 4b). Experiments have suggested that this may be an artefact of having a wider or sharper seiche peak. Therefore, the method is not perfect, although it does clearly demonstrate the dependence of period on depth. A number of previous authors have also noted such a dependence but have not gone so far as to estimate the effective depth from measurements of period (e.g. Ichiye and Dowling, 1960; Okihiro et al., 1993; de Jong et al., 2003; Park et al., 2015).

The numerical model has proved to be a useful tool for understanding why inlets such as Lerwick Harbour, Balta Sound or Sullom Voe resonate at particular periods and in indicating the spatial scales of such resonances. Developments in modelling using higher-frequency meteorological information and improved coastal bathymetry can be expected in the future. For example, the importance to seiche generation of air pressure jumps, rapid changes in wind direction and wind gusts remain to be properly investigated. In addition, longer model runs than the two short ones available to the present study are to be anticipated.

The extensive set of sea level information from Lerwick has enabled us to study two large events (in 2008 and 2015) in some detail that appear to have resulted from the long waves associated with meteotsunamis occurring in summer months. Similar events, often clearly connected to thunderstorms or heavily precipitating convective systems, are known to have occurred elsewhere in the region, such as on the coasts of Denmark, where they are called 'summer waves' (Huess, 2001), and Germany (Newig, 2015), and in the English Channel (Tappin et al., 2013; Williams et al., 2018). Therefore, they are likely to be more frequent than one might have previously thought. Long (2015) refers to a number of examples of possible meteotsunamis around the UK coast which have sometimes been interpreted as tsunamis. Otherwise, most large seiche events will be a result of winter storms. The long sea level record from Lerwick has allowed us to consider how such seiche activity occurs within each year and from year to year (Table 3).

One intriguing aspect of the data concerns the existence of seiches in several records with periods of approximately half an hour. We have no explanation of why this is the case, other than that period necessarily follows from the typical length and depth of inlets around Shetland. Our numerical model suggests that local resonances with periods such as this will be found in several inlets, notably in Lerwick Harbour, Balta Sound, Burra Firth and Dury Voe, which are confirmed for those locations for which we have measurements. We have no evidence to support the hypothesis of a coherent east-facing shelf resonance with half-hour period as proposed by Cartwright and Young (1974), preferring instead a simpler explanation in terms of individual (but approximately simultaneous) local resonances, an explanation which Cartwright and Young (1974) rejected.

However, seiches with many other periods are found elsewhere around Shetland. For example, an energetic seiche with a period of approximately 81 minutes is found at Sella Ness in the important inlet of Sullom Voe on the northwest coast of the Shetland mainland, as previously identified by Dooley (1981). Considerable energy is contained in the seiche observed at Busta House centred on a period of 48 minutes. This particular seiche is not represented well in our numerical model, probably due to inadequacy of the EMODnet bathymetric data set for the mainland west coast. However, as explained above, its period is consistent with general knowledge of the Swarbacks Minn/Busta Voe inlet. All of these seiches are almost certainly consequences of resonance of the inlets concerned, high-frequency sea level variability on the outer islands (Out Skerries and Fair Isle in the present data set, and Foula reported by Cartwright and Young, 1974) having much lower amplitudes than around the three main islands of Shetland.

On a different topic, with regard to the anomalously large amplitude for M12 observed at Balta Sound by Cartwright and Young (1974) and confirmed by us, our recent data from Gutcher contradicts their theory for its source as being tidal ringing of the northwest shelf. It indicates that the spatial distribution of the 12<sup>th</sup> diurnals is more complicated than the authors proposed.

In summary, our Shetland measurements have provided a demonstration of how seiches with many different periods and amplitudes can be found within one group of islands. We know they are not unique. For example, similarly large seiches are known to occur at Stornoway in the Hebrides (e.g. at the end of January 2016 when Lerwick also experienced large seiches, Figure 13). We believe that seiches will be endemic along almost any coastline where suitable forcings exist and where the topography of the coastline or harbour lends itself to resonances of one kind or another. And yet seiches are a much under-researched aspect of sea level science. Most sea level scientists average over high-frequency variability in order to obtain the hourly, daily and monthly values that they need for the study of tides, storm surges and long-term sea level change. In fact, as we have shown in the case of Shetland, seiches can have amplitudes of many decimetres, and so deserve to be better understood within studies of sea level variability. In particular, as Vilibić and Šepić (2017) have

recommended, such high-frequency variability, including that of seiches, needs to be taken into account properly in research into extreme sea levels. In addition, even though the amplitudes of seiches may be small, the currents associated with them can be large enough to require consideration when designing marine infrastructure (e.g. fish farms or tidal power turbines in the case of Shetland). Therefore, we would encourage the study of seiches at as many locations around the world as possible, making use of both measurements and models, leading to the compilation of a 'seiche climatology' for the world coastline that could be used in coastal applications.

#### Acknowledgements

We thank James Phillips of Shetland Islands Council and Christopher Rich of Unst for their help with this project. We are also grateful to Charlie Smith at the Lerwick Port Authority and David Parnaby of the Fair Isle Bird Observatory. Les Bradley, Peter Foden, Jeff Pugh, Angela Hibbert and Judith Wolf from the National Oceanography Centre in Liverpool provided valuable support and advice. In addition, we thank John Penman from the UK Met Office for meteorological data from the Lerwick weather station. Our fieldwork in Shetland was largely funded by the Crown Estate. Some of the figures in this paper were generated using the Generic Mapping Tools (Wessel and Smith, 1998). All tide gauge and model data sets discussed in this paper will be lodged with BODC. We are grateful to three anonymous reviewers and to the editor Dr. A.B. Rabinovich for their suggestions on improvements to drafts of the paper.

## References

- Airy, G.B. (1878). On the tides at Malta. *Philosophical Transactions of the Royal Society of London*, 169, 123-138, doi:10.1098/rstl.1878.0006.
- Blackman, D.L., Graff, J., & Vassie, J.M. (1981). Tidal currents in Yell Sound and the outer regions of Sullom Voe. *Proceedings of the Royal Society of Edinburgh*, 80B, 73-90, doi:10.1017/S0269727000006503.
- Burt, S. (2007). The lowest of the lows ... Extremes of barometric pressure in the British Isles, Part 1 - the deepest depressions. *Weather*, 62, 4-14, doi: 10.1002/wea.20.
- Cartwright, D.E., & Young, C.M. (1974). Seiches and tidal ringing in the sea near Shetland. *Proceedings of the Royal Society of London, A*, 338, 111-128, doi:10.1098/rspa.1974.0077.
- Cartwright, D.E., Edden, A.C., Spencer, R., & Vassie, J.M. (1980). The tides of the northeast Atlantic Ocean. *Philosophical Transactions of the Royal Society of London, A*, 298, 87-139, doi:10.1098/rsta.1980.0241.
- Chrystal, G. (1906). On the hydrodynamical theory of seiches. *Transactions of the Royal Society of Edinburgh - Earth and Environmental Science*, 41, 599-649, doi:10.1017/S0080456800035523.
- Chrystal, G.C. (1910). Seiches and other oscillations of lake-surfaces, observed by the Scottish Lake Survey. pp.29-90 in Bathymetrical survey of the fresh water lochs of Scotland, Volume 1, (eds. J. Murray and L. Pullar). Edinburgh: Challenger Office, 6 volumes.
- Copernicus Climate Change Service (C3S) (2017). ERA5: Fifth generation of ECMWF atmospheric reanalyses of the global climate. Copernicus Climate Change Service Climate Data Store (CDS). Accessed January 2019, <https://cds.climate.copernicus.eu/cdsapp#!/home>.
- Danish Hydrographic Institute (DHI) (2010). MIKE 21 flow model (FM) hydrodynamic and transport modules. Documentation available from [http://manuals.mikepoweredbydhi.help/2017/MIKE\\_21.htm](http://manuals.mikepoweredbydhi.help/2017/MIKE_21.htm).
- Dee, D.P. and 35 others. (2011). The ERA-Interim reanalysis: configuration and performance of the data assimilation system. *Quarterly Journal of the Royal Meteorological Society*, 137, 553-597, doi:10.1002/qj.828.
- de Jong, M.P.C., Holthuijsen, L.H., & Battjes, J.A. (2003). Generation of seiches by cold fronts over the southern North Sea. *Journal of Geophysical Research*, 108(C4), 3117, doi:10.1029/2002JC001422.
- Donn, W. L., & Wolf, D. M. (1972). Seiche and water level fluctuations in Grindavik Harbor, Iceland. *Limnology and Oceanography*, 17, 639-643.
- Dooley, H.D. (1981). Oceanographic observations in Sullom Voe, Shetland in the period 1974-1978. *Proceedings of the Royal Society of Edinburgh*, 80B, 55-71, doi:10.1017/S0269727000006497.
- Egbert, G.D., Bennett, A.F., & Foreman, M.G.G. (1994). TOPEX/POSEIDON tides estimated using a global inverse model. *Journal of Geophysical Research Oceans*, 99, 24321-24852, doi:10.1029/94JC01894.

Flynn, D. (1973). The topography of the seafloor around Orkney and Shetland and in the northern North Sea. *Journal of the Geological Society*, 129, 39-59, doi:10.1144/gsjgs.129.1.0039.

Forel, F.-A. (1876). Note sur un limnimètre enregistreur établi a Morges pour étudier les seiches. *Annales de Chimie et de Physique, 5th series, Volume 9*, 90-92.

Forel, F.-A. (1901). Handbuch der Seenkunde: Allgemeine Limnologie. Stuttgart, Germany: J. Engelhorn.

Golmen, L. G., Molvaer, J., & Magnusson, J. (1994). Sea level oscillations with super-tidal frequency in a coastal embayment of western Norway. *Continental Shelf Research*, 14, 1439–1454, doi:10.1016/0278-4343(94)90084-1.

Halliday, R. (2011). Shetland Islands wave and tidal resource. Report No. 805\_NPC\_SIC\_004 prepared for Shetland Islands Council. Available from [https://www.shetland.gov.uk/planning/documents/805\\_NPC\\_SIC\\_R\\_004-LowRes.pdf](https://www.shetland.gov.uk/planning/documents/805_NPC_SIC_R_004-LowRes.pdf).

Huess, V. (2001). Sea level variations in the North Sea from tide gauges, altimetry and modelling. PhD Thesis, University of Copenhagen (October 2000). Danish Meteorological Institute Scientific Report 01-08. 93pp.

Ichiye, T., & Dowling, D.B. (1960). A note on the seiches of Alligator Harbor, Florida. *The Journal of the Oceanographical Society of Japan*, 16(3), 7-17.

Inman, D., Munk, W., & Balay, M. (1962). Spectra of low frequency ocean waves along the Argentine shelf. *Deep Sea Research*, 8, 153-164, doi:10.1016/0146-6313(61)90018-1.

Jenkins, G.M., & Watts, D.G. (1968). Spectral analysis and its applications. Merrifield, Virginia: Holden-Day. 525pp.

Lerwick Port Authority (LPA) (2018). Information for visiting yachts. <https://www.lerwick-harbour.co.uk/assets/files/2018-yacht-pack.pdf>.

Long, D. (2015). A catalogue of tsunamis reported in the UK. British Geological Survey Internal Report, IR/15/043. 63pp.

National Library of Scotland (NLS) (1924). Admiralty chart for the Shetland Islands, Part 1 (1118a). Available from [https://maps.nls.uk/coasts/admiralty\\_charts\\_list.html](https://maps.nls.uk/coasts/admiralty_charts_list.html).

National Library of Scotland (NLS) (1927). Admiralty chart for the Shetland Islands, Part 2 (1118b). Available from [https://maps.nls.uk/coasts/admiralty\\_charts\\_list.html](https://maps.nls.uk/coasts/admiralty_charts_list.html).

Newig, J. (2015). Historische "seebären"/meteotsunamis an den deutschen küsten - mit einem schwerpunkt Sylt. pp.87-104 in, Aktuelle Küstenforschung an der Nordsee (ed. T. Tillmann), Coastline Reports, 25 (2015). Wilhelmshaven: The Coastal Union Germany. ISSN 0928-2734, ISBN 978-3-939206-18-7.

Okiihiro, M., Guza, R.T., & Seymour, R.J. (1993). Excitation of seiche observed in a small harbor. *Journal of Geophysical Research*, 98(C10), 18201-18211, doi:10.1029/93JC01760.

Park, J., Sweet, W.V., & Heitsenrether, R. (2015). Water level oscillations in Monterey Bay and Harbor. *Ocean Science*, 11, 439-453, doi:10.5194/os-11-439-2015.

Park, J., MacMahan, J., Sweet, W.V., & Kotun, K. (2016). Continuous seiche in bays and harbors. *Ocean Science*, 12, 355-368, doi:10.5194/os-12-355-2016.

Pugh, D.T, & Woodworth, P.L. (2014). Sea-level science: Understanding tides, surges, tsunamis and mean sea-level changes. Cambridge: Cambridge University Press. ISBN 978-1-107-02819-7. 395pp.

Rabinovich, A.B. (2009). Seiches and harbor oscillations. In, Handbook of Coastal Engineering (ed. Y.C. Kim), pp. 193–236. Hackensack, New Jersey: World Scientific Publishing, doi:10.1142/9789812819307\_0009.

Rossiter, J.R. (1971). Long period sea waves: seiches, surges and tides in coastal waters. pp.155-169 (Chapter 11) in, Dynamic Waves in Civil Engineering (eds. Howells, D.A., Haigh, I.P. and Taylow, C.). London: Wiley-Interscience.

Šepić, J., Vilibić, I., Lafon, A., Macheboeuf, L. & Ivanović, Z. (2015) High-frequency sea level oscillations in the Mediterranean and their connection to synoptic patterns. *Progress in Oceanography*, 137, 284-298. doi:10.1016/j.pocean.2015.07.005.

Sibley, A., Cox, D., Long, D., Tappin, D., & Horsburgh, K. (2016). Meteorologically generated tsunami-like waves in the North Sea on 1/2 July 2015 and 28 May 2008. *Weather*, 71, 68-74, doi:10.1002/wea.2696.

Sorensen, R. M. (1978). Basic coastal engineering. Hoboken, New Jersey: John Wiley.

Tappin, D.R., Sibley, A., Horsburgh, K., Daubord, C., Cox, D., & Long, D. (2013). The English Channel 'tsunami' of 27 June 2011 – a probable meteorological source. *Weather*, 68, 144-152, doi:10.1002/wea.2061.

Tucker, M.J. (1963). Long waves in the sea. *Science Progress*, 51 (No. 203), 413-424.

Vilibić, I., Šepić, J., Rabinovich, A.B., & Monserrat, S. (2016) Modern approaches in meteotsunami research and early warning. *Frontiers in Marine Science*, 3:57, doi: 10.3389/fmars.2016.00057.

Vilibić, I., & Šepić, J. (2017). Global mapping of nonseismic sea level oscillations at tsunami timescales. *Scientific Reports*, 7:40818, doi:10.1038/srep40818.

Weatherall, P., Marks, K.M., Jakobsson, M., Schmitt, T., Tani, S., Arndt, J.E., Rovere, M., Chayes, D., Ferrini, V., & Wigley, R. (2015). A new digital bathymetric model of the world's oceans. *Earth and Space Science*, 2, 331-345, doi:10.1002/2015EA000107.

Wessel, P., & Smith, W.H.F. (1998). New, improved version of Generic Mapping Tools released. *Eos, Transactions of the American Geophysical Union*, 79, 579.

Williams, D.A., Horsburgh, K.J., Schultz, D.M., & Hughes, C.W. (2018). Examination of generation mechanisms for an English Channel meteotsunami: combining observations and modelling. *Journal of Physical Oceanography*, 49, 103-120, doi: 10.1175/JPO-D-18-0161.1.

Wilson, B.W. (1972). Seiches. *Advances in Hydroscience*, 8, 1–94.



Wolf, J., Yates, N., Brereton, A., Buckland, H., De Dominicis, M., Gallego, A., & Murray, R.O. (2015). The Scottish shelf model. Part 1: Shelf-wide domain. *Marine Scotland Science*, doi:10.7489/1692-1. Available at [www.gov.scot](http://www.gov.scot).

Woodworth, P.L., Pugh, D.T., Meredith, M.P., & Blackman, D.L. (2005). Sea level changes at Port Stanley, Falkland Islands. *Journal of Geophysical Research*, 110, C06013, doi:10.1029/2004JC002648.

Woodworth, P.L. (2017). Seiches in the eastern Caribbean. *Pure and Applied Geophysics*, 174(12), 4283-4312, doi:10.1007/s00024-017-1715-7.

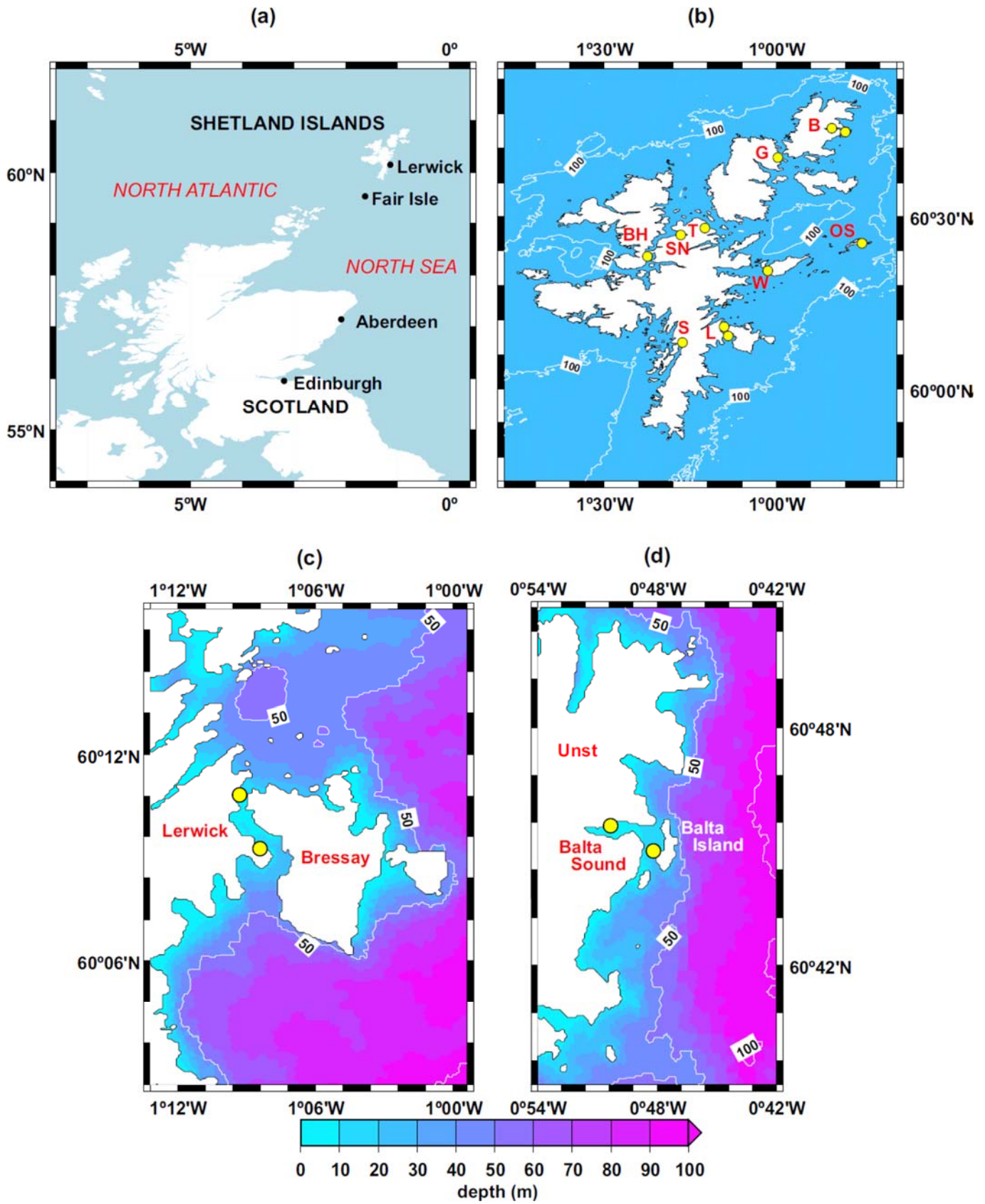


Figure 1 (a) The Shetland Islands in relation to the Scottish mainland. (b) Bathymetry around Shetland from GEBCO/EMODnet, indicating the limit of the continental shelf by the 100m depth contour, and measurement sites shown by yellow dots: L, Lerwick with two sites (Lerwick and Lerwick North); B, Baltasound with two sites (Balta Pier and Balta Offshore to the west and east respectively); BH, Busta House; W, Whalsay; T, Toft; G, Gutcher; S, Scalloway; SN, Sella Ness; OS, Out Skerries. An additional measurement site at Fair Isle is off the map to the south. Lerwick, Busta House, Toft, Scalloway and Sella Ness are located on the Shetland mainland; Gutcher on the island of Yell to the north; and Baltasound on the island of Unst further north. (c) Lerwick Harbour, the location of which is shown by L in the southeast part of (b), with yellow dots indicating the locations of the permanent bubbler tide gauge at its southwest corner and the temporary Lerwick North gauge towards the north end of the northern entrance. (d) Balta Sound, the location of which is shown by B in the northeast part of (b), with yellow dots indicating the positions of temporary gauges at Balta Pier on the north coast of Balta Sound and Balta Offshore deployed in approximately 12 m of water off the west coast of Balta Island and near to the main entrance of Balta Sound. (c) and (d) indicate the bathymetry as used in the numerical model, with the 50 and 100 m contours labelled.

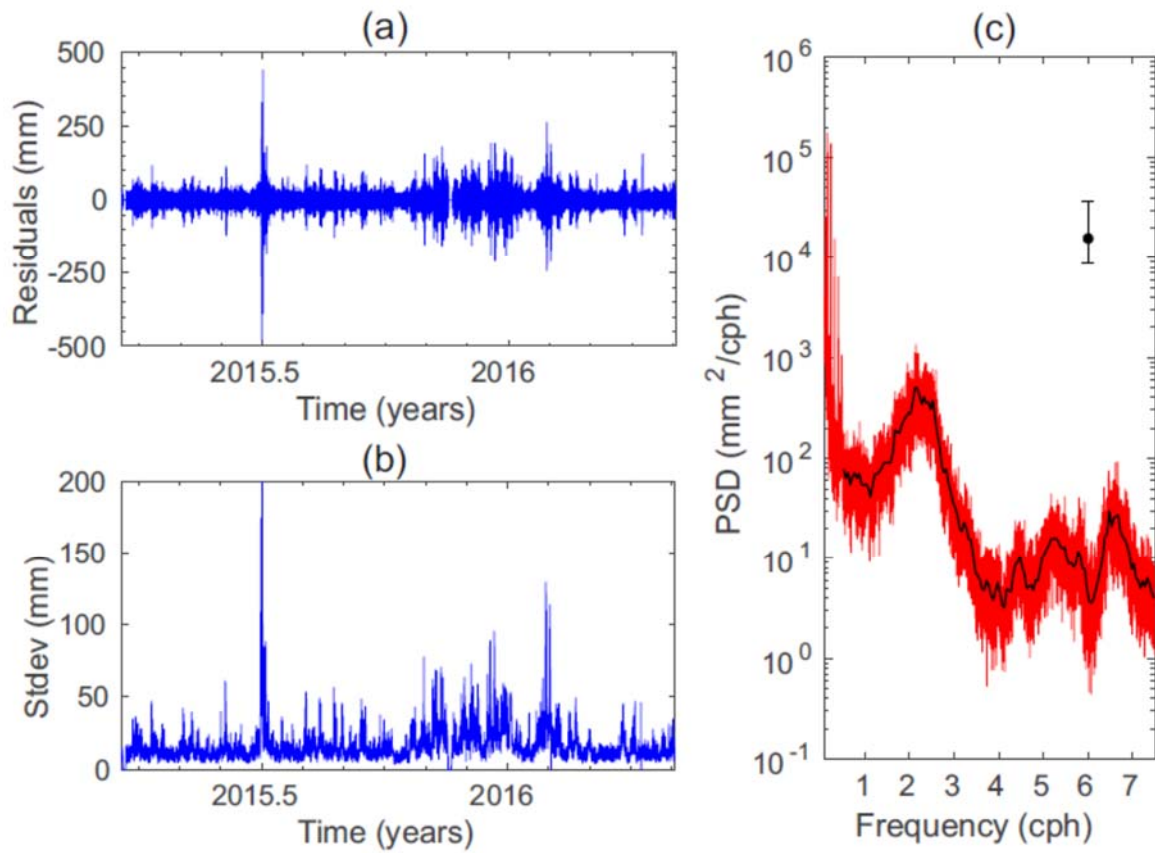


Figure 2. Sea level variability at Lerwick (corresponding figures for all stations may be found in the Supplementary Material). (a) Time series of residuals computed as described in the text. (b) The standard deviation of this high-frequency residual variability within 2-hour sections of data. (c) Power spectral density (PSD) of total sea level variability (red). The figure starts at 0.1 cph in order to cut off the large peaks of the diurnal and semidiurnal tides and the error bar indicates 95% confidence level. The black curve presents a low-pass filtered version of the spectrum above 0.5 cph obtained by smoothing into bins of 0.05 cph.

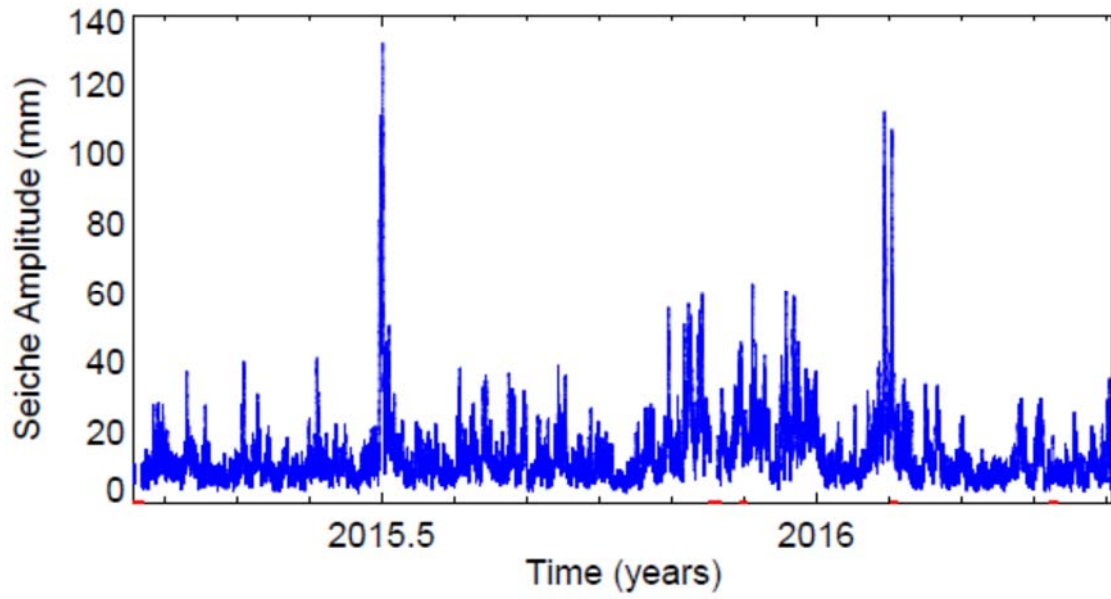


Figure 3. Amplitude of the '28-min seiche' at Lerwick for March 2015 – May 2016 using the 'window-regression' method. Red dots indicate short data gaps.

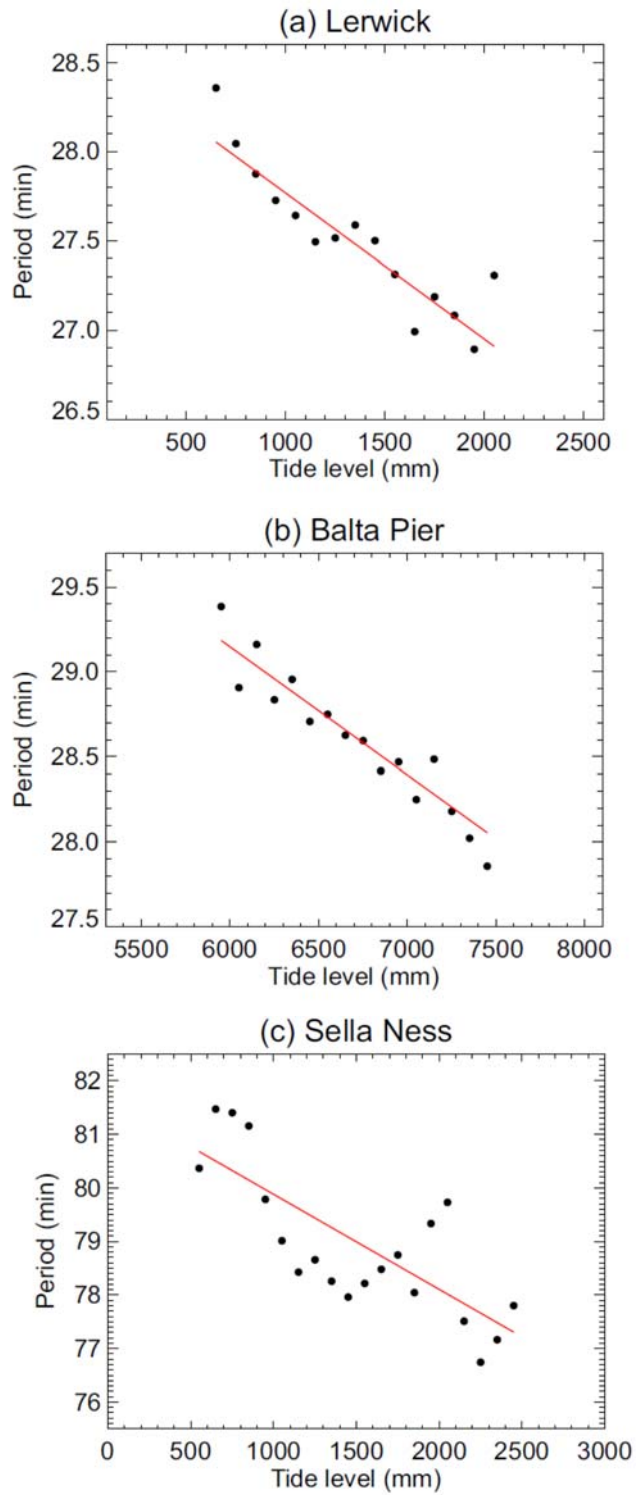


Figure 4. Period of the '28-minute' seiche observed in 6-hour windows as a function of the average sea level (in effect the average tide level) during the window using data from (a) Lerwick and (b) Balta Pier. And of the '81-minute' seiche at Sella Ness (c). 'Tide level' in these figures refers to the local datum at each station and has no relevance between stations.

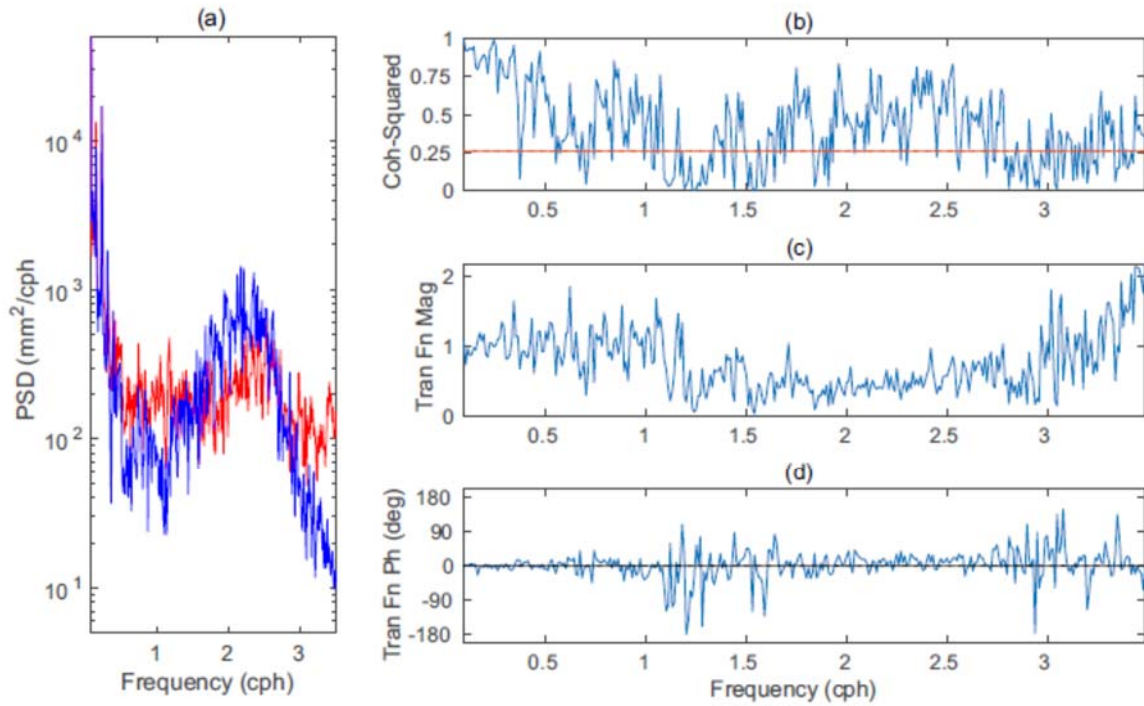


Figure 5. (a) Power spectral density (PSD) for Lerwick (blue) and Lerwick North (red) in the overlapping period of operation. (b) Magnitude-squared coherence between them. (c) Transfer function magnitude (Lerwick North compared to Lerwick). (d) Transfer function phase. The red line in (b) indicates 95% confidence level following Jenkins and Watts (1968).

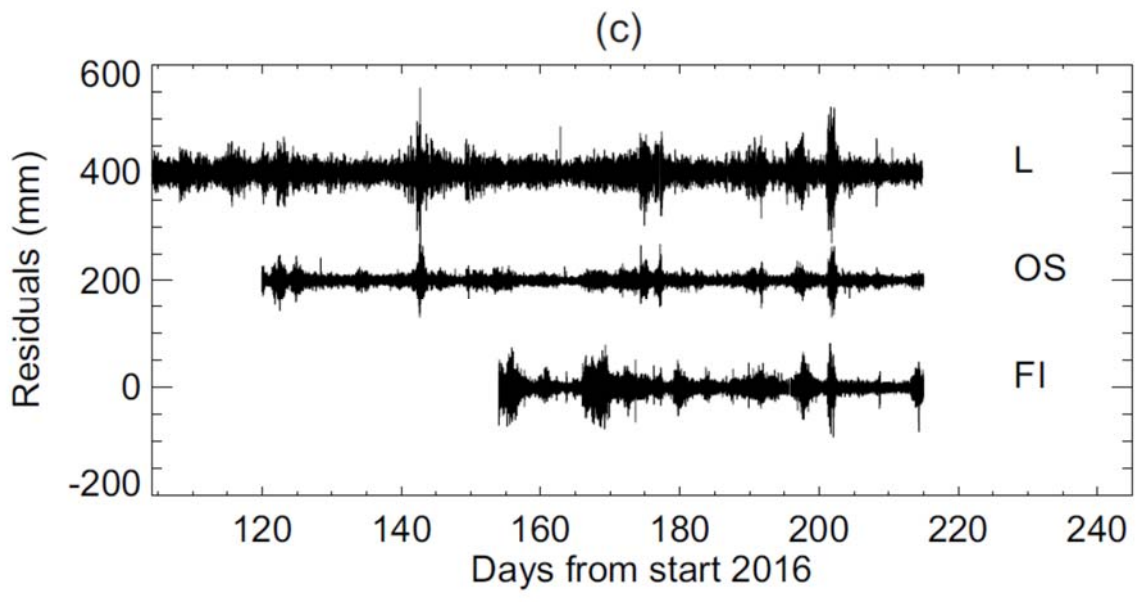
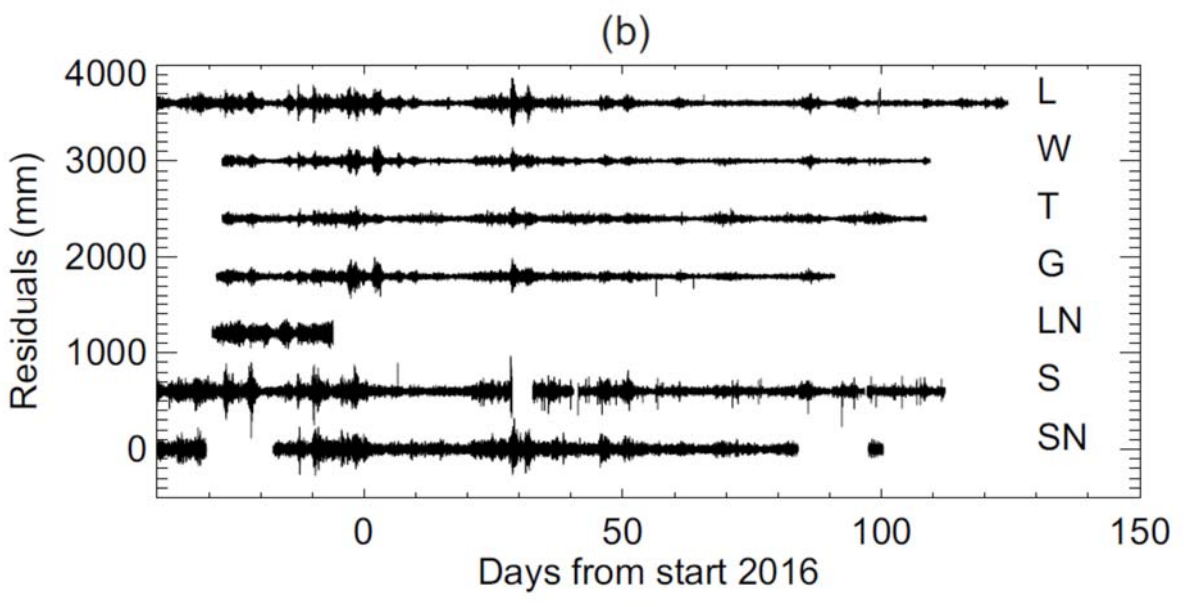
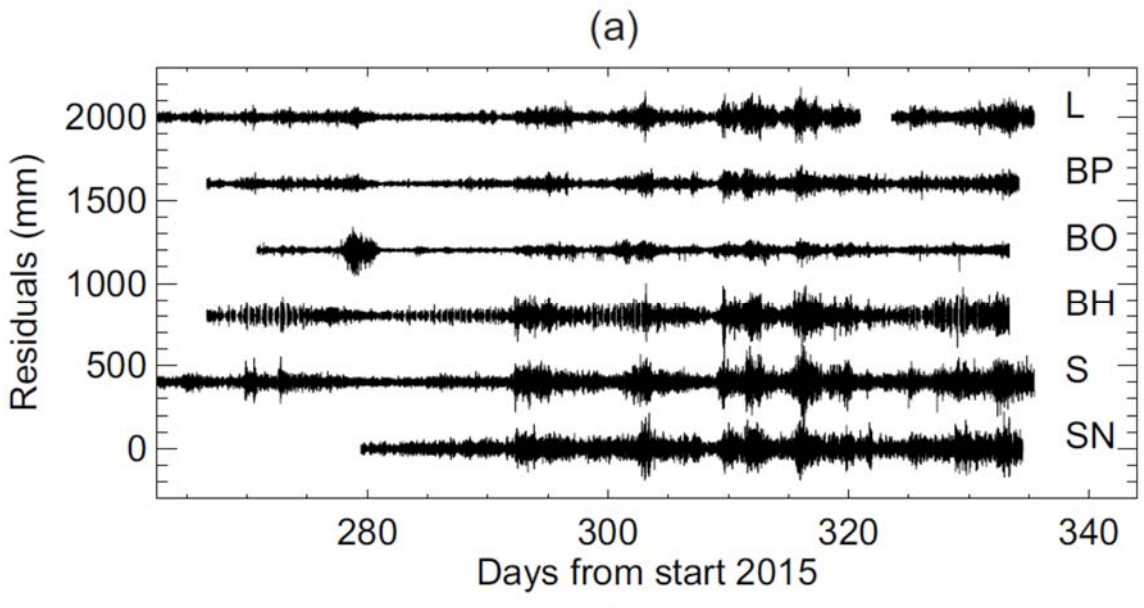




Figure 6. (a) Time series of residuals for tide gauge recordings up to December 2015. (b) Recordings during December 2015 to April 2016. (c) Recordings during April-August 2016. Stations are identified by the codes given in Figure 1(b) and Table 1. Each time series has been offset for presentation purposes.

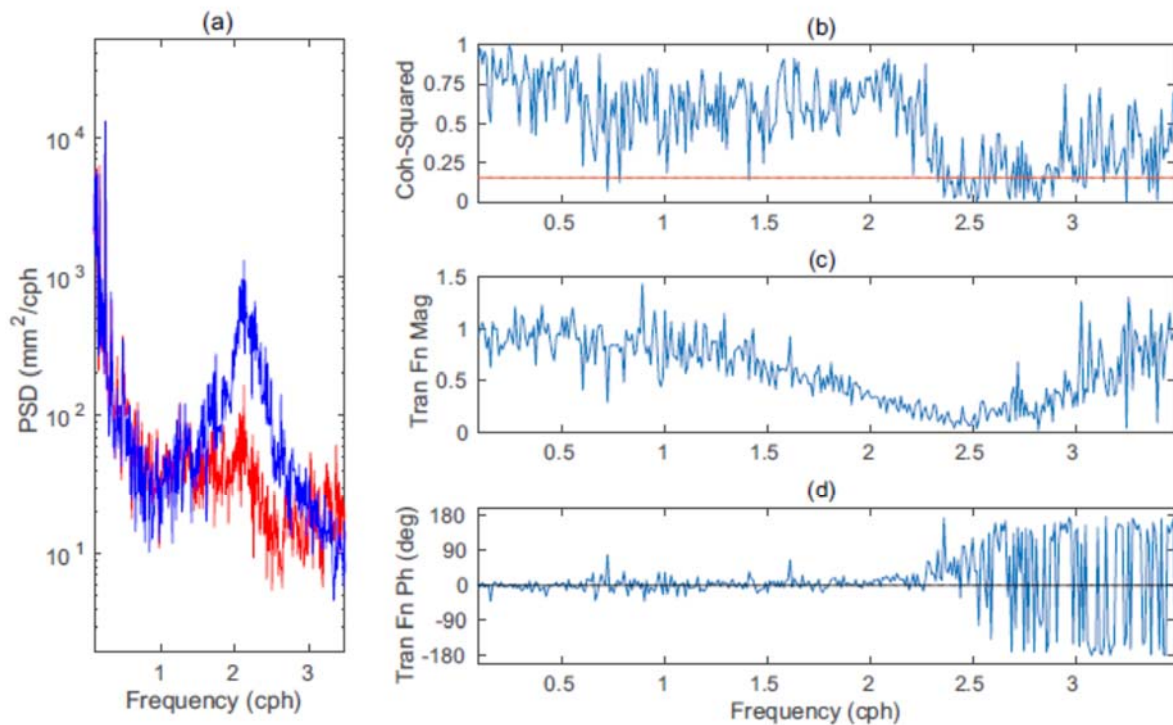


Figure 7. (a) Power spectral density (PSD) for Balta Pier (blue) and Balta Offshore (red) in the overlapping period of operation. (b) Magnitude-squared coherence between them. (c) Transfer function magnitude (Balta Offshore compared to Balta Pier). (d) Transfer function phase. The red line in (b) indicates 95% confidence level following Jenkins and Watts (1968).

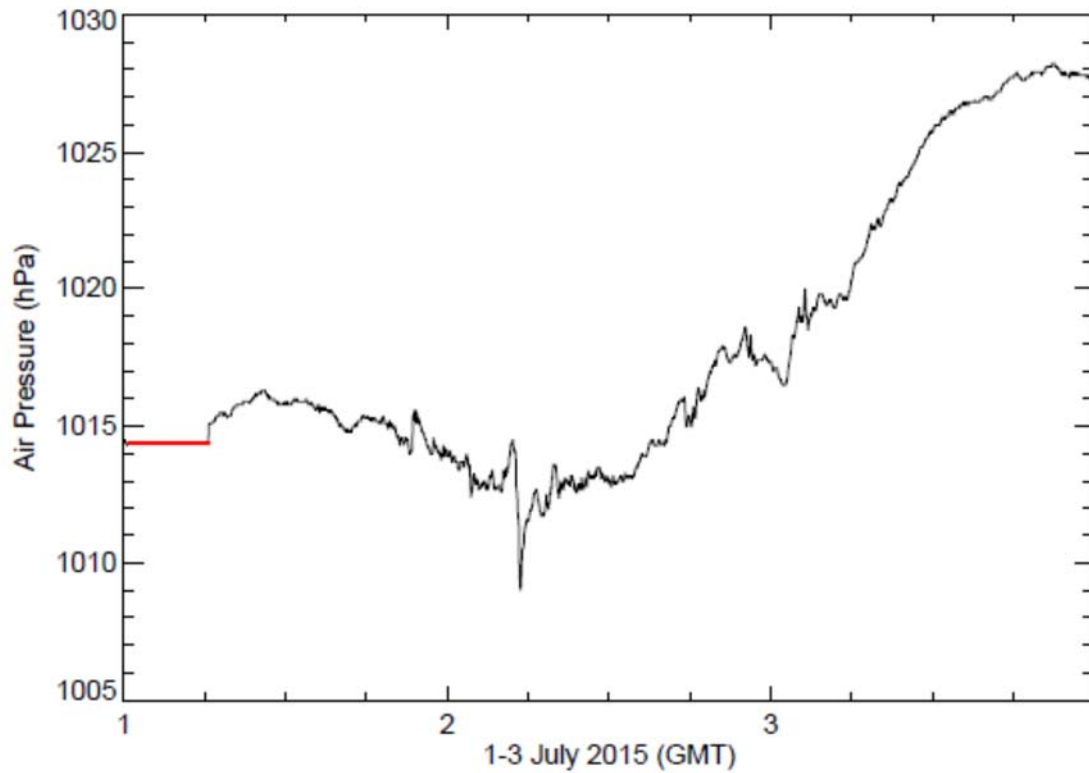


Figure 8. Surface air pressure (1-min values) at Lerwick during 1-3 July 2015. The red dots at the start indicate missing values.

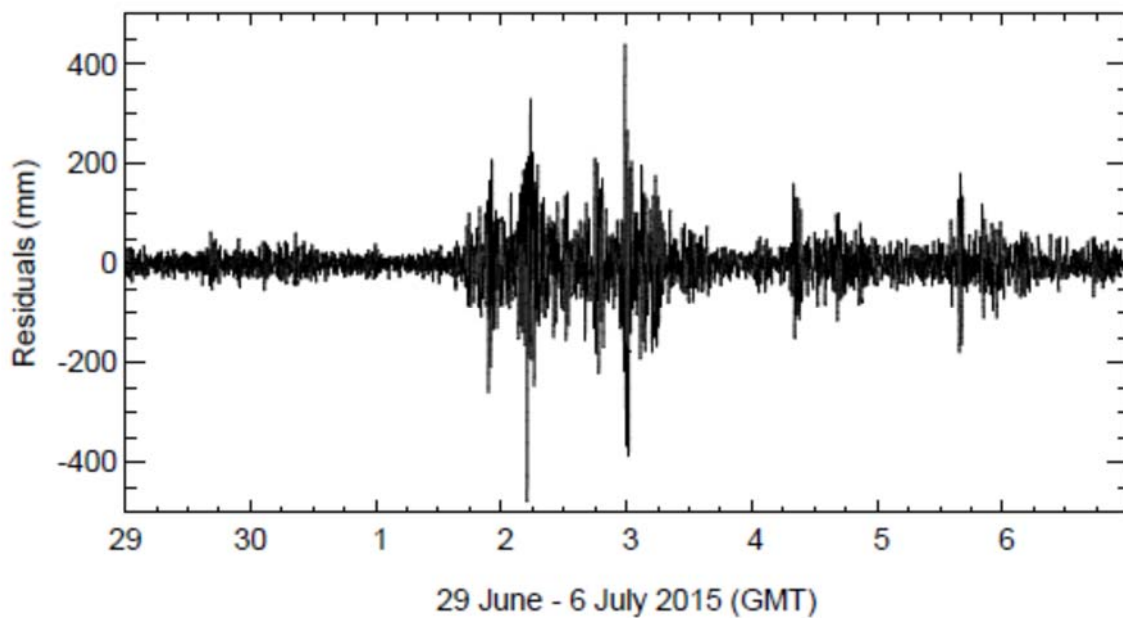


Figure 9. Sea level residuals at Lerwick during 29 June – 6 July 2015.

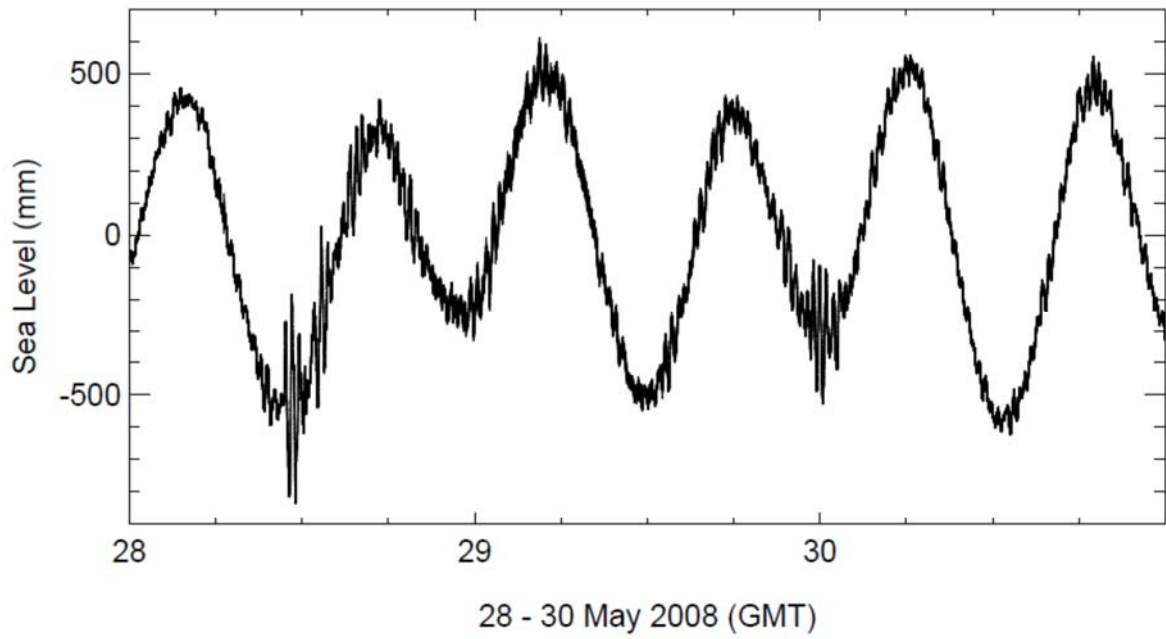
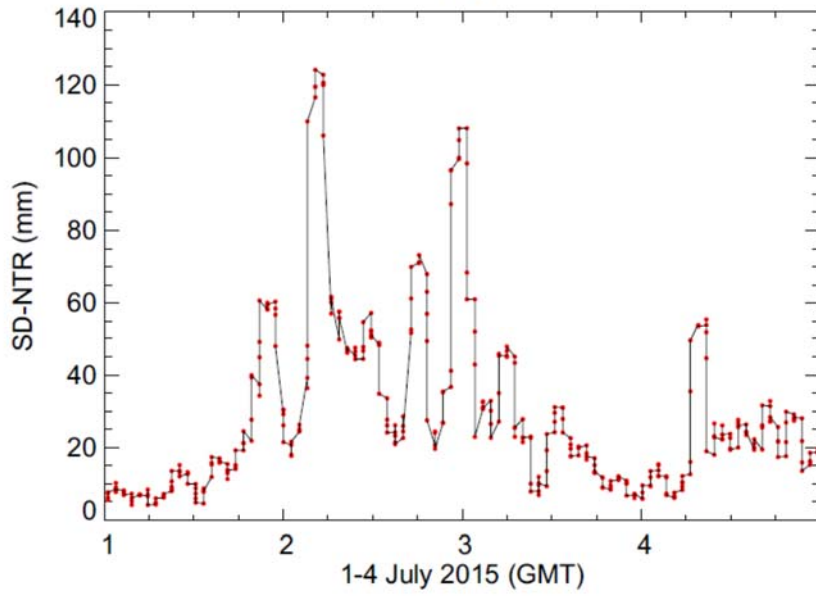
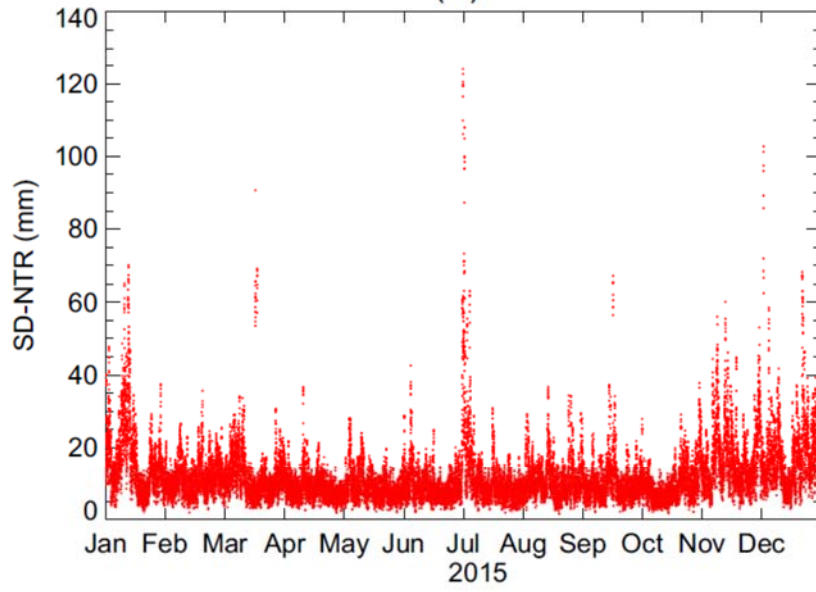


Figure 10. The Lerwick tidal record for 28-30 May 2008 showing periods of seiche superimposed on the tide.

(a)



(b)



(c)

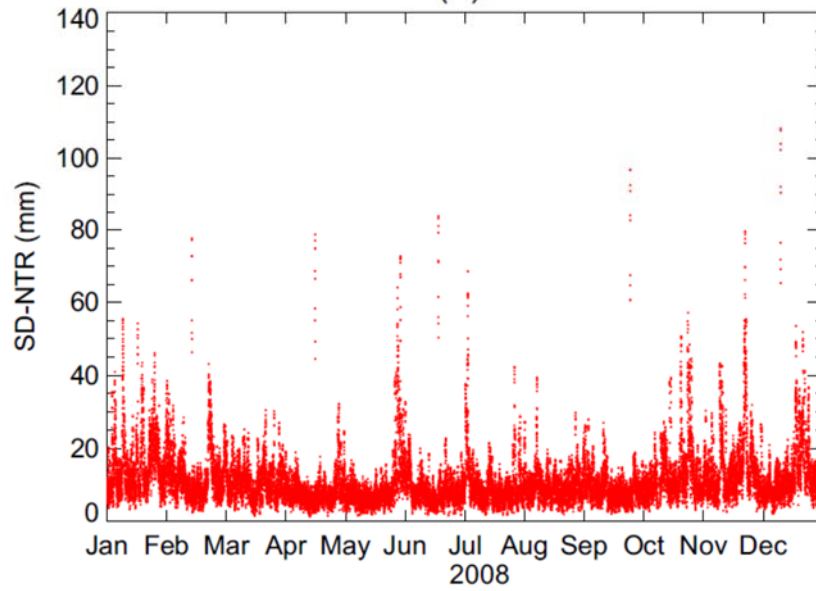


Figure 11. Standard deviation of 15-min non-tidal residuals (SD-NTR) within windows containing 9 15-min values at Lerwick for (a) 1-4 July 2015, (b) 2015, and (c) 2008. There is one red dot for each window; dots in (a) have been connected to aid visualisation.

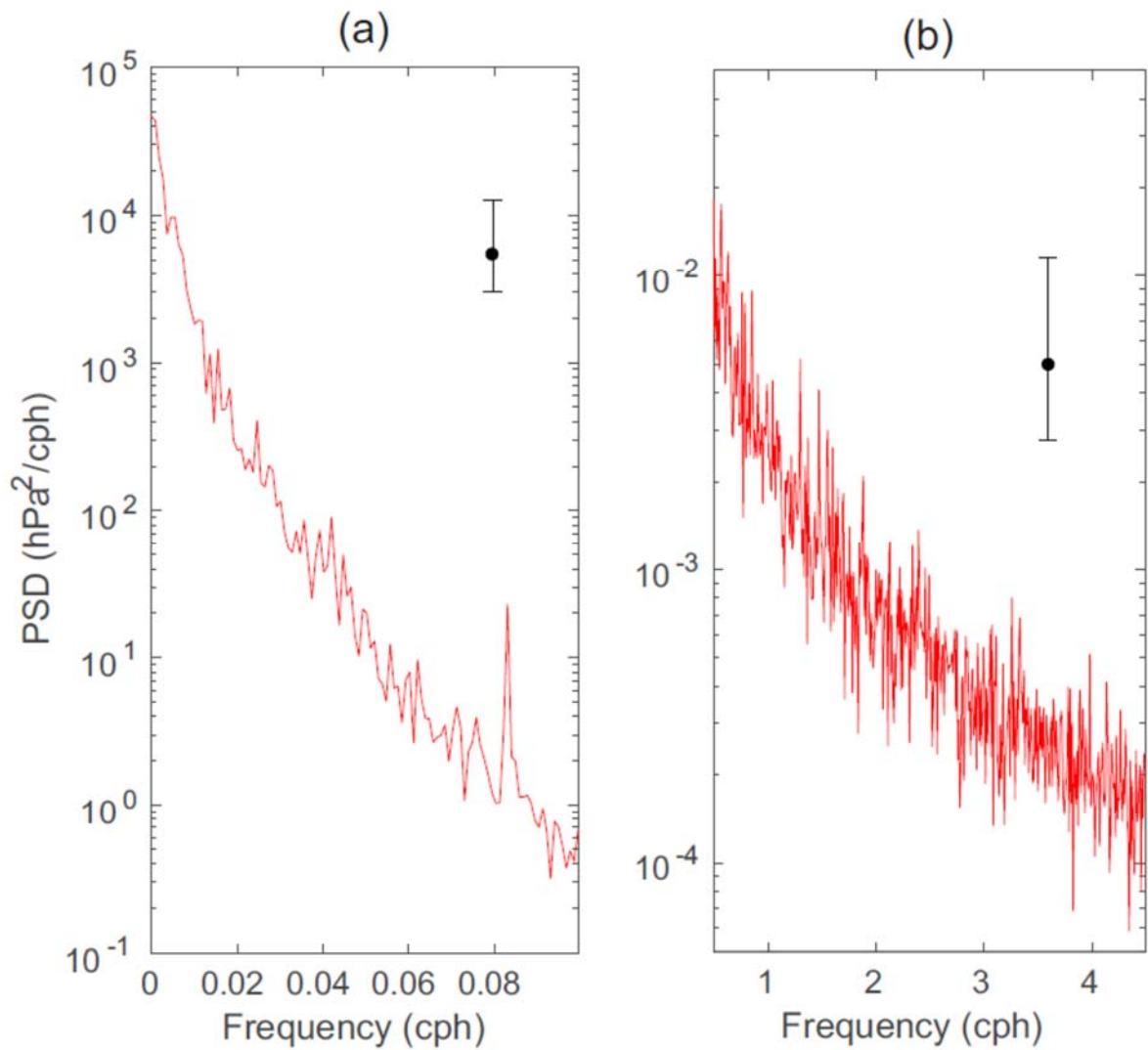
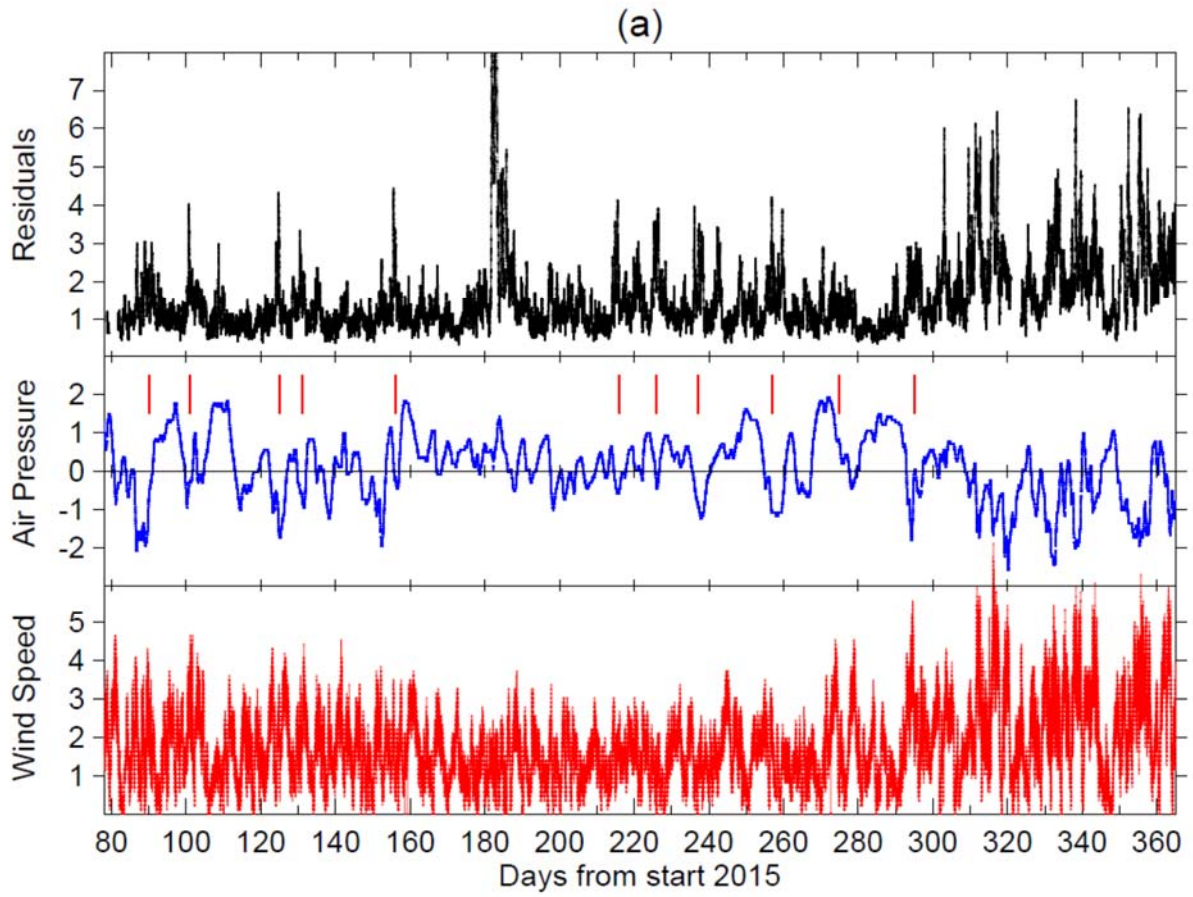


Figure 12. Power spectral density (PSD) of sea level air pressure at Lerwick obtained from 1-minute values during 2014-2015. (a) The low frequency part of the spectrum showing the peak at S2 (0.0833  $\text{cph}$ ), and (b) for 0.5-4.5  $\text{cph}$ , being the range of frequency of interest regarding seiches at Lerwick. The error bars are 95% confidence level estimates.



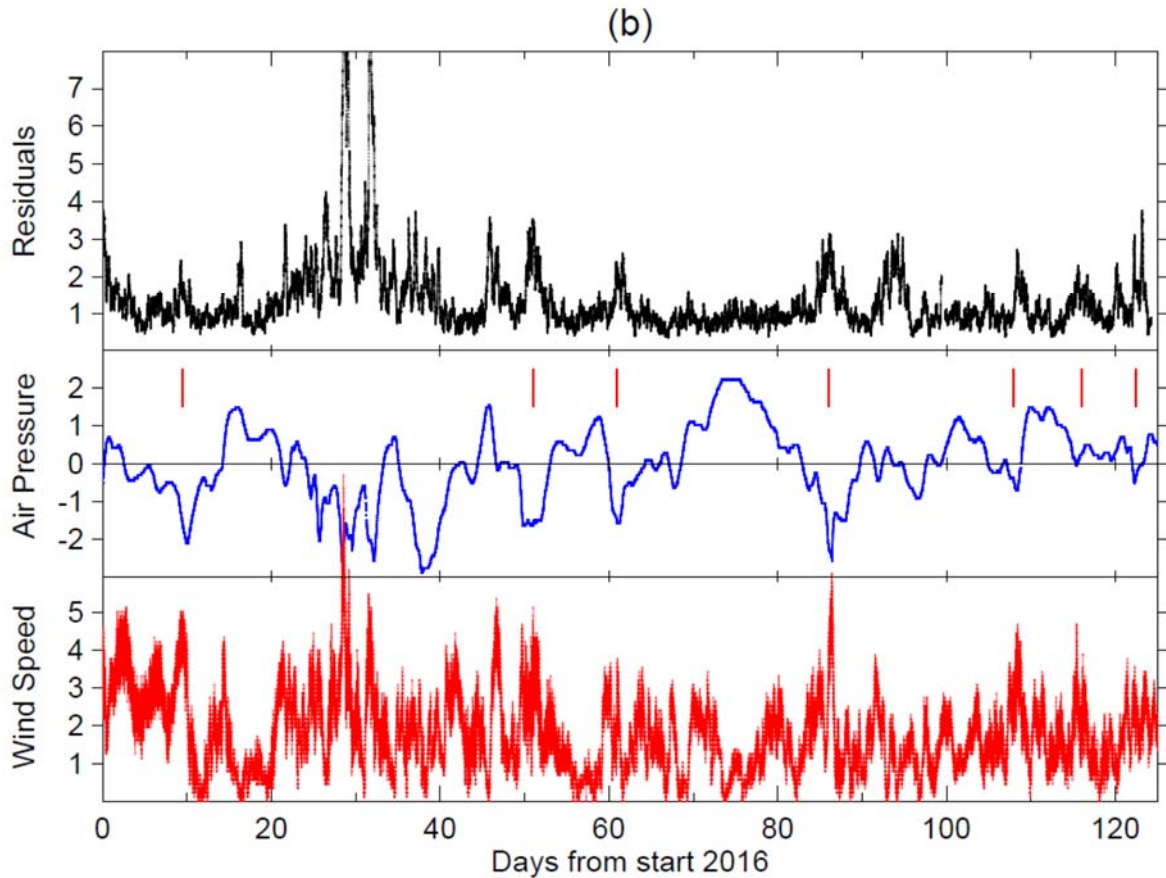


Figure 13. (top) Amplitude of the '28-min seiche' at Lerwick (as in Figure 3) divided by the standard deviation of its time series; (middle) surface air pressure at Lerwick (minus its average value) also scaled by its standard deviation; (bottom) wind speed similarly scaled. The red dashes indicate events for which we have associated periods of seiche activity and the passage of depressions shown on synoptic charts. (a) for 2015, (b) for 2016. Note that the large seiche amplitudes of July 2015 and January 2016 exceed the upper plot limits.

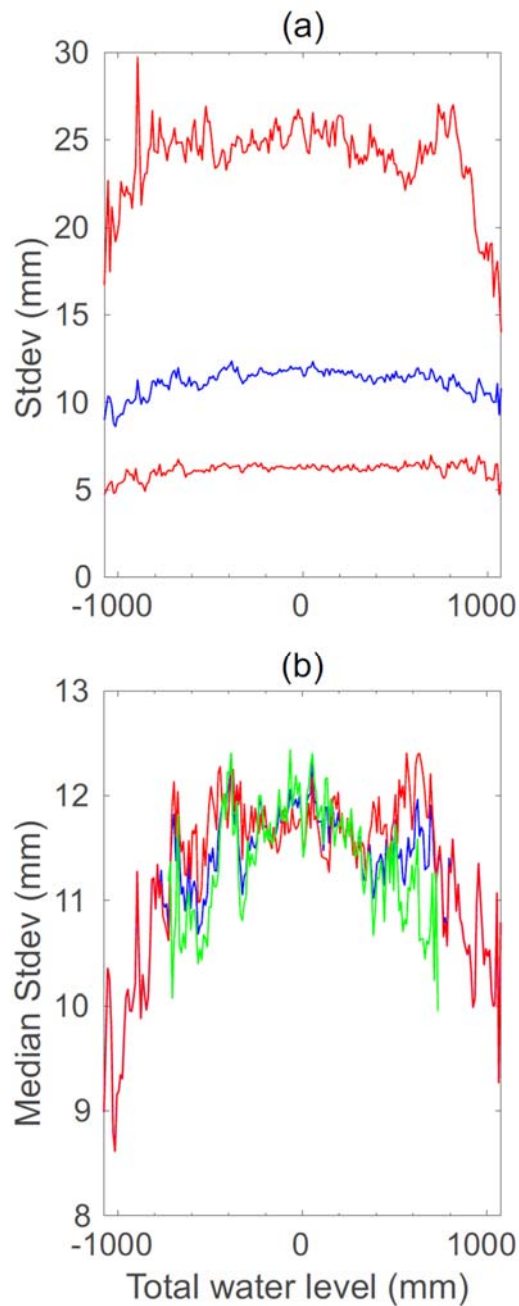


Figure 14. (a) Median standard deviation of filtered (1.5-3 cph so selecting the '28-min band') residuals within 2-hour windows through the Lerwick record as a function of the height of the tide (blue). 90- and 10-percentile standard deviations are shown in red. (b) The median curve for the whole record (blue) and for tidal range above (red) and below (green) the mean tidal range (i.e. periods of spring and neap tides). (a) demonstrates a dependence of standard deviation on the tide at high and low waters, at least for the median and 90-percentile distributions, whereas (b) exhibits little difference between spring and neap tides (see text).



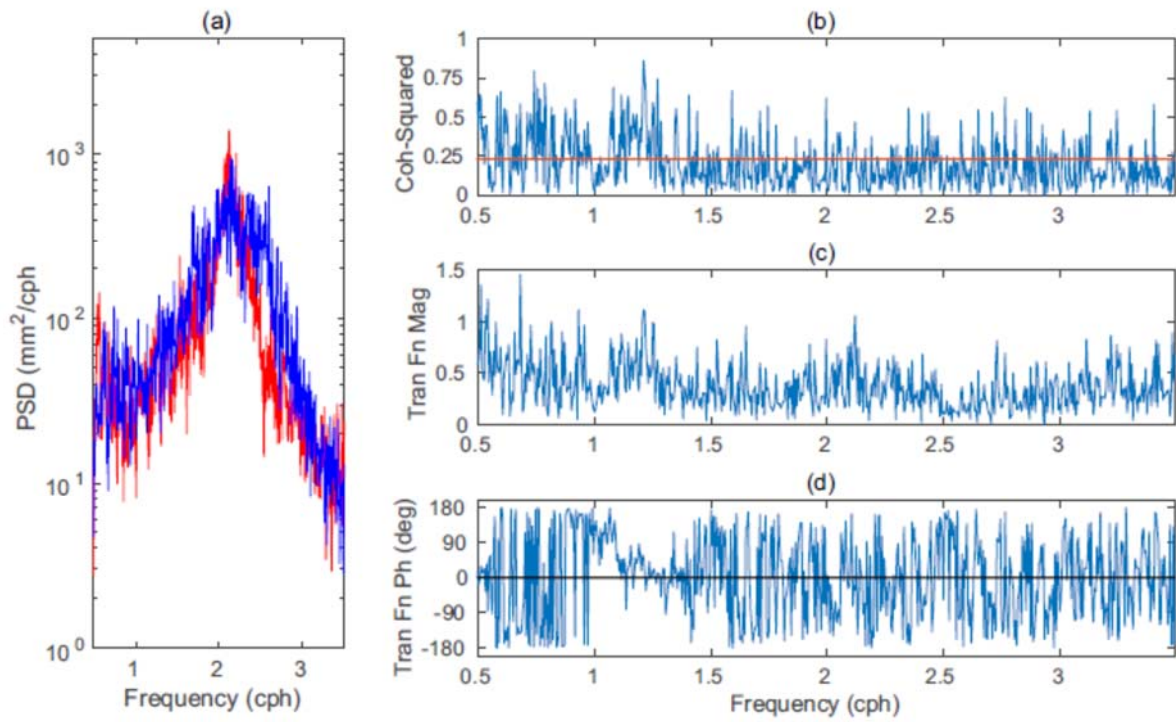


Figure 15. (a) Power spectral density (PSD) of residuals at Lerwick (blue) and Balta Pier (red) for their overlapping period of operation (Figure 4a). (b) Magnitude-squared coherence between them. (c) Transfer function magnitude (Balta Pier compared to Lerwick). (d) Transfer function phase. The red line in (b) indicates 95% confidence level following Jenkins and Watts (1968).

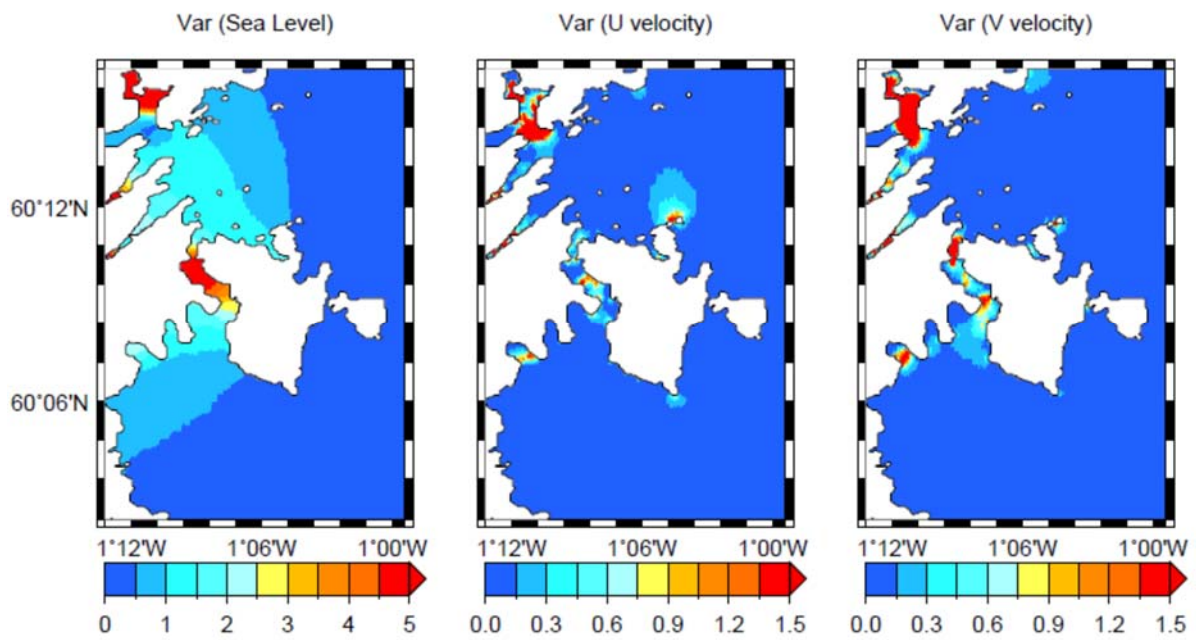


Figure 16. Variance of sea level, zonal and meridional components of current (denoted U and V respectively) for Lerwick Harbour from the July 2015 numerical model run. (Those for the January 2015 run are similar). Units are  $\text{cm}^2$  and  $(\text{cm}/\text{sec})^2$ . Model time series have been band-pass filtered to isolate variability within the 25-35 minute band (see Supplementary Material Set C). See the Supplementary Figures D(xiv-xvii) for examples of variance at Balta Sound, Burra Firth, Dury Voe, Sella Ness and Blue Mull Sound.

Table 1. Summary of tide gauge data.

Location	West/East Coast	Latitude (°N) and Longitude (°W)	Sensor	Data span (month/year) and [sampling]
Lerwick (L)	E	60.154 1.140	Sea level from Environment Agency bubbler pressure gauge	3/15 – 8/16 [1 min] (*) (**)
Balta Pier (BP)	E	60.759 0.839	RBR total pressure (NOC)	9/15 – 12/15 [RBR]
Balta Offshore (BO)	E	60.747 0.800	RBR total pressure (NOC)	9/15 – 12/15 [RBR]
Busta House (BH)	W	60.384 1.374	RBR total pressure (NOC)	9/15 – 12/15 [RBR]
Whalsay (W)	E	60.342 1.025	RBR total pressure (NOC)	12/15 - 4/16 [RBR]
Toft (T)	E	60.467 1.208	RBR total pressure (NOC)	12/15 - 4/16 [RBR]
Gutcher (G)	E	60.673 0.996	RBR total pressure (NOC)	12/15 - 4/16 [RBR]
Lerwick North (LN)	E	60.181 1.151	Sea level from vented pressure sensor (NOC)	12/15 – 2/16 [3 min spot]
Scalloway (S)	W	60.135 1.272	Sea level from Shetland Islands Council pressure gauge	6/15 – 4/16 [1 min] (**)
Sella Ness (SN)	W	60.447 1.278	Sea level from Shetland Islands Council pressure gauge	10/15 – 4/16 [1 min] (**)
Out Skerries (OS)	To the East	60.423 0.751	RBR total pressure (NOC)	4/16-8/16 [RBR]
Fair Isle (FI)	To the South	59.538 1.604	RBR total pressure (NOC)	4/16-8/16 [RBR]

(\*) Lerwick bubbler data were acquired at 1 Hz and averaged into 1-min values for the period shown. 15-min averages are available for 1993 onwards.

(\*\*) In these cases the dates shown are the data spans used for this paper. Lerwick data are ongoing. Some fragmentary earlier and later data are also available for Scalloway and Sella Ness.

[RBR] indicates a sampling of 10-second averages every 3 minutes.

Table 2. Characteristics of each record: Column 2 shows the frequencies and corresponding periods of the main spectral peaks (all frequencies listed are above 1 cph except for Sella Ness), with peaks mentioned in the text underlined. Frequencies are shown in cph to two decimal places using the method described in the text, and converted to periods in units of tenths of a minute. Column 3 shows the standard deviations of the residuals shown in Figure 6.

Location	Main spectral peaks: Frequency (cph) and Period (min)	Standard deviation of residuals in Figure 6(a-c) (mm)
Lerwick (L)	<u>2.14</u> , 4.46, 5.19, 6.46 <u>28.1</u> , 13.5, 11.6, 9.3	(a) 21, (b) 22, (c) 14
Balta Pier (BP)	<u>2.11</u> , 4.79, 6.54 <u>28.4</u> , 12.5, 9.2	19
Balta Offshore (BO)	1.26, <u>2.11</u> , 3.24, 4.04, 4.46, 5.94, 6.74, 7.29 47.5, <u>28.4</u> , 18.5, 14.9, 13.5, 10.1, 8.9, 8.2	15
Busta House (BH)	<u>1.26</u> , 2.21, 2.79, 3.71, 5.31, 6.21, 6.94, 7.46 <u>47.5</u> , 27.1, 21.5, 16.2, 11.3, 9.7, 8.7, 8.0	34
Whalsay (W)	1.24, <u>1.76</u> , 2.99, 3.81, 4.81, 5.64, 6.14, 7.34 48.5, <u>34.0</u> , 20.1, 15.7, 12.5, 10.6, 9.8, 8.2	16
Toft (T)	<u>1.11</u> , <u>2.39</u> , 3.06, 4.09, 4.44, 4.94, 6.51, 7.46 <u>53.9</u> , <u>25.1</u> , 19.6, 14.7, 13.5, 12.2, 9.2, 8.0	17
Gutcher (G)	<u>1.44</u> , 2.09, 3.09, 4.11, 4.91, 5.36, 5.86, 6.76, 7.34 41.7, 28.7, 19.4, 14.6, 12.2, 11.2, 10.2, 8.9, 8.2	20
Lerwick North (LN)	1.19, <u>2.51</u> , 3.39, 4.49, 5.56, 6.41, 7.09 50.5, <u>23.9</u> , 17.7, 13.4, 10.8, 9.4, 8.5	36
Scalloway (S)	<u>1.34</u> , 2.84, 3.59, 5.44, 6.34 <u>44.9</u> , 21.2, 16.7, 11.0, 9.5	(a) 30, (b) 31
Sella Ness (SN)	<u>0.74</u> , 2.14, 4.04, 5.21, 7.09 <u>81.4</u> , 28.1, 14.9, 11.5, 8.5	(a) 35, (b) 35
Out Skerries (OS)	1.41, 2.89, 3.41, 3.99, 5.16, 6.86 42.5, 20.8, 17.6, 15.1, 11.6, 8.7	7
Fair Isle (FI)	1.89, 2.99, 3.49, 4.16, 5.19, 5.89, 7.09 31.8, 20.1, 17.2, 14.4, 11.6, 10.2, 8.5	11

Table 3. Years in the Lerwick record that are at least 85% complete (completeness shown in column 2), for which there are the number of windows shown with SD-NTR above the specified threshold (column 3), separated into 'winter' and 'summer' halves of the year (columns 4 and 5). The ratio of the winter to total numbers is given in column 6. There are  $365 \times 24 \times 4 = 35040$  windows, each centred on nine 15-min values, in a normal year.

Threshold 30 mm

1993	1.000	1001	896	105	0.895
1994	1.000	811	542	269	0.668
1995	0.997	480	391	89	0.815
1996	0.969	500	154	346	0.308
1997	0.998	861	482	379	0.560
1999	0.852	912	675	237	0.740
2004	0.996	454	342	112	0.753
2005	0.996	879	694	185	0.790
2006	0.864	289	182	107	0.630
2008	0.997	850	654	196	0.769
2009	0.993	433	215	218	0.497
2010	0.858	181	72	109	0.398
2012	0.988	290	225	65	0.776
2013	1.000	707	508	199	0.719
2014	1.000	555	346	209	0.623
2015	0.994	977	763	214	0.781

Threshold 60 mm

1993	1.000	112	103	9	0.920
1994	1.000	76	56	20	0.737
1995	0.997	36	30	6	0.833
1996	0.969	104	27	77	0.260
1997	0.998	100	62	38	0.620
1999	0.852	111	94	17	0.847
2004	0.996	60	45	15	0.750
2005	0.996	59	39	20	0.661
2006	0.864	51	47	4	0.922
2008	0.997	65	26	39	0.400
2009	0.993	57	31	26	0.544
2010	0.858	21	8	13	0.381
2012	0.988	32	20	12	0.625
2013	1.000	75	47	28	0.627
2014	1.000	52	19	33	0.365
2015	0.994	104	58	46	0.558